2020 Spring

Advanced Solidification

06.03.2020

Eun Soo Park

Office: 33-313
Telephone: 880-7221
Email: espark@snu.ac.kr
Office hours: by appointment

Undercooling ΔT_0

$$\Delta T_0 = \Delta T_r + \Delta T_D \quad \Rightarrow \quad \Delta G_{total} = \Delta G_r + \Delta G_D \quad \Rightarrow \quad v = k_2 D \frac{\Delta T_0}{\lambda}\left(1 - \frac{\lambda^*}{\lambda}\right)$$

Curvature — Composition gradient

$\Delta G_r = \dfrac{2\gamma_{\alpha\gamma} V_m}{\lambda}$ → *free energy dissipated in forming α/β interfaces*

ΔG_D → *free energy dissipated in diffusion*

By varying the interface undercooling (ΔT_0) it is possible to vary the growth rate (V) and spacing (λ) independently.

Therefore, it is impossible to predict the spacing that will be observed for a given growth rate. However, controlled growth experiments show that a specific value of λ Is always associated with a given growth rate.

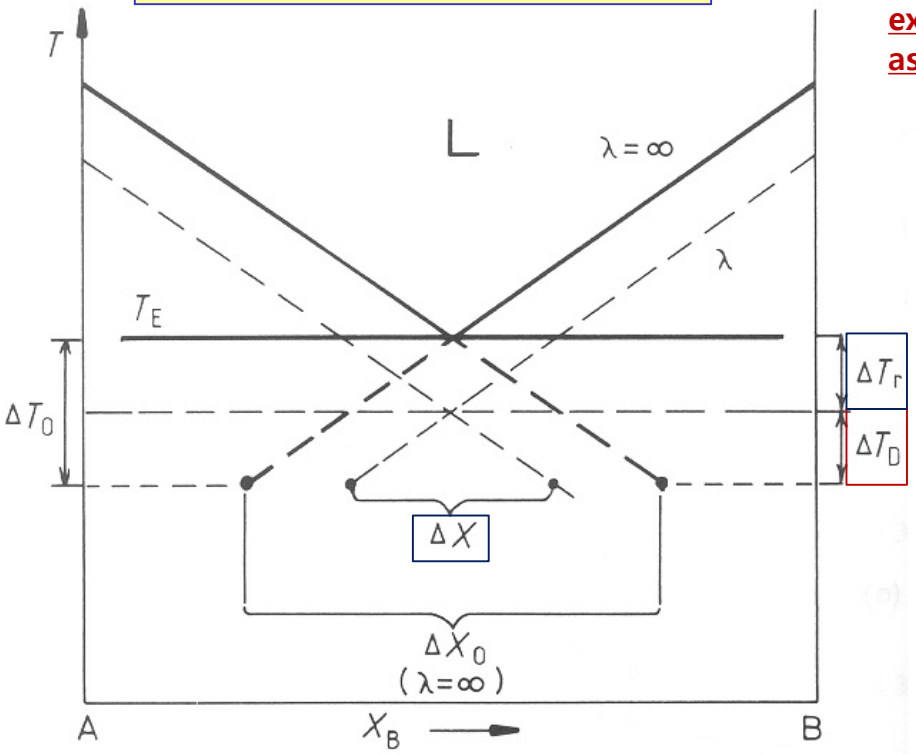

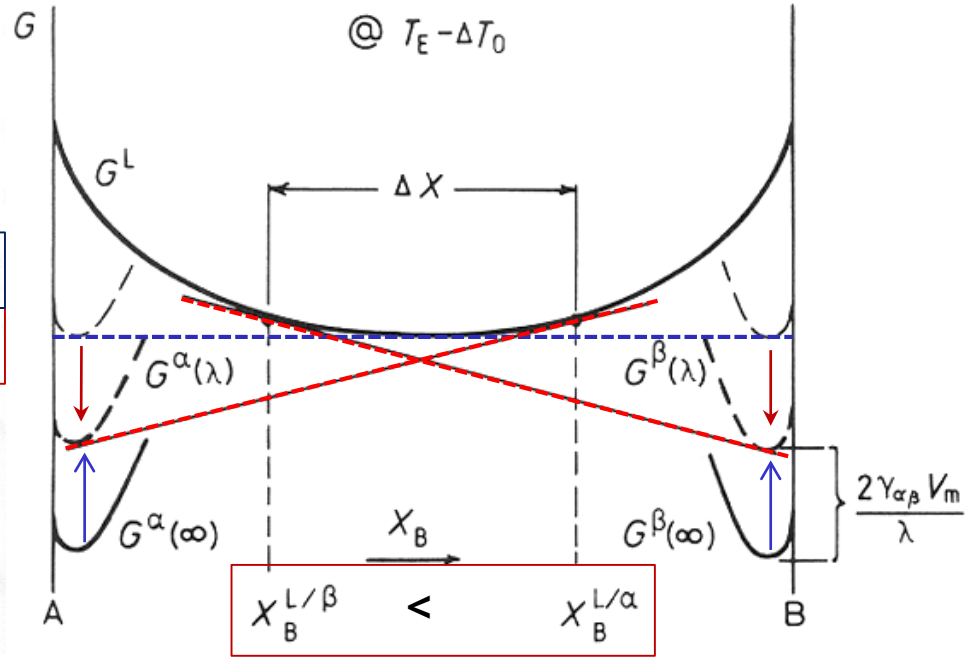

Fig. 4.34 Eutectic phase diagram showing the relationship between ΔX and ΔX_0 (exaggerated for clarity)

Undercooling ΔT_0

$$\Delta T_0 = \Delta T_r + \Delta T_D$$

Curvature Composition gradient

$$\Delta G_{total} = \Delta G_r + \Delta G_D$$

$$v = k_2 D \frac{\Delta T_0}{\lambda}\left(1 - \frac{\lambda^*}{\lambda}\right)$$

By varying the interface undercooling (ΔT_0) it is possible to vary the growth rate (V) and spacing (λ) independently.

$$\Delta G_r = \frac{2\gamma_{\alpha\gamma} V_m}{\lambda}$$

→ *free energy dissipated in forming α/β interfaces*

$\Delta G_D \rightarrow$ *free energy dissipated in diffusion*

Therefore, it is impossible to predict the spacing that will be observed for a given growth rate. However, controlled growth experiments show that a specific value of λ Is always associated with a given growth rate.

*** For example,**

Maximum growth rate at a fixed ΔT_0 $\rightarrow \lambda_0 = 2\lambda^*$

(4) $v = k_2 D \frac{\Delta T_0}{\lambda}\left(1 - \frac{\lambda^*}{\lambda}\right)$ → $v_0 = k_2 D \Delta T_0 / 4\lambda^*$ **(5)**

From Eq. 4.39 $\lambda^* = +\frac{2T_E \gamma V_m}{\Delta H \Delta T_0}$ → $\Delta T_0 \propto 1/\lambda^*$ **(6)**

So that the following relationships are predicted:

(5) + (6) →

$$v_0 \lambda_0^2 = k_3 \text{ (constant)}$$

$$\frac{v_0}{(\Delta T_0)^2} = k_4$$

Ex) Lamellar eutectic in the Pb-Sn system

$k_3 \sim 33\ \mu m^3/s$ and $k_4 \sim 1\ \mu m/s \cdot K^2$

→ $v = 1\ \mu m/s$, $\lambda_0 = 5\ \mu m$ and $\Delta T_0 = 1\ K$

* Total Undercooling

$$\Delta T_0 = \Delta T_r + \Delta T_D$$

Strictly speaking,

ΔT_i term should be added but, negligible for high mobility interfaces

Driving force for atom migration across the interfaces

ΔT_r: Undercooling required to overcome the interfacial curvature effects

ΔT_D: Undercooling required to give a sufficient composition difference to drive the diffusion

$\Delta T_D \rightarrow$ Vary continuously from the middle of the α to the middle of the β lamellae

$\Delta T_0 = const$ ← Interface is essentially isothermal.

$\Delta T_D \rightarrow \Delta T_r$ The interface curvature will change across the interface.

Should be compensated

* A planar eutectic front is not always stable.

Binary eutectic alloys contains impurities or other alloying elements ➡ "Form a cellular morphology"

analogous to single phase solidification

restrict in a sufficiently high temp. gradient.

➡ The solidification direction changes as the cell walls are approached and the lamellar or rod structure fans out and may even change to an irregular structure.

➡ Impurity elements (here, mainly copper) concentrate at the cell walls.

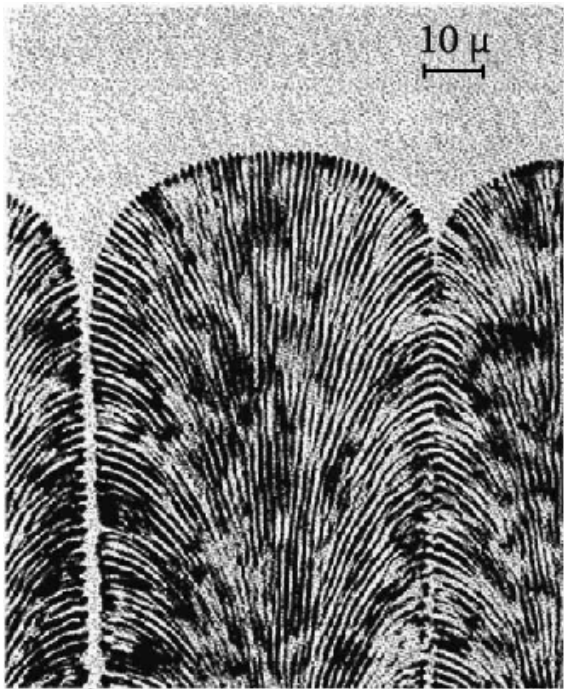

A planar eutectic front is not always stable.

Binary eutectic alloys contains impurities or other alloying elements ➡ "Form a cellular morphology" analogous to single phase solidification restrict in a sufficiently high temp. gradient.

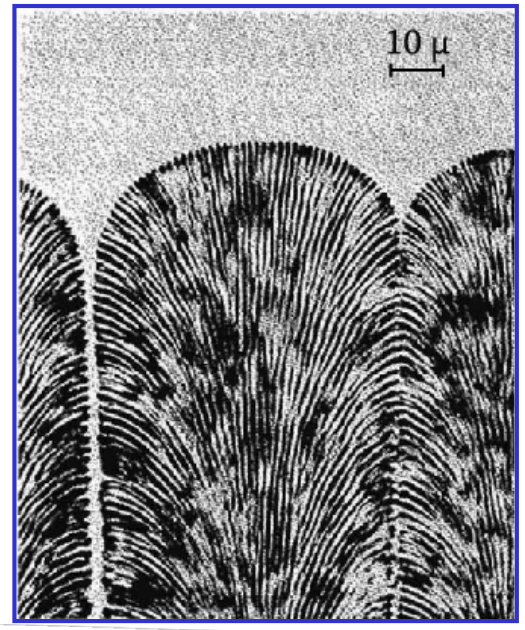

➡ The solidification direction changes as the cell walls are approached and the lamellar or rod structure fans out and may even change to an irregular structure.

➡ Impurity elements (here, mainly copper) concentrate at the cell walls.

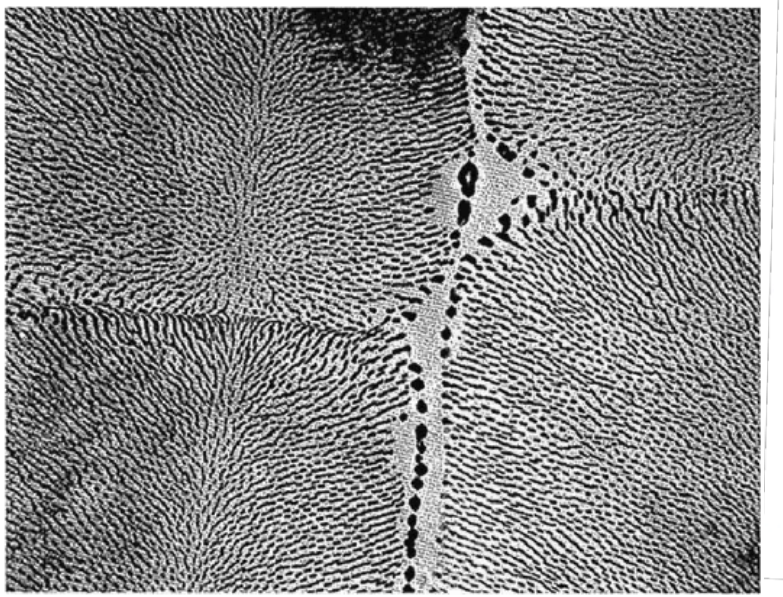

Fig. 4.35 Transverse section through the cellular structure of an Al-Al_6Fe rod eutectic (x3500).

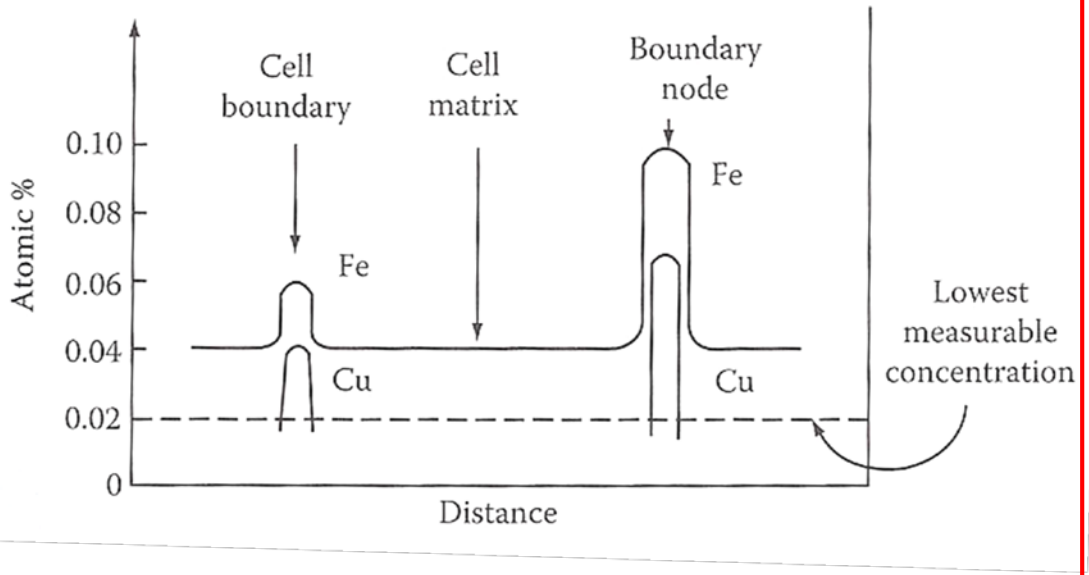

Fig. 4.36 Composition profiles across the cells in Fig. 4.35b.

An alternative approach for lamellar growth by Jackson and Chalmers,

Terminating layer T
by change of speed of growth

The stability of the tip T is the criterion for the stable lamellar width, λ.

Assumption:

1) interface ~ isothermal
2) Total supercooling of interfaces
   ~ sum of the supercooling due to curvature
3) the enrichment of the liquid in contact with the interface by rejection of the solute

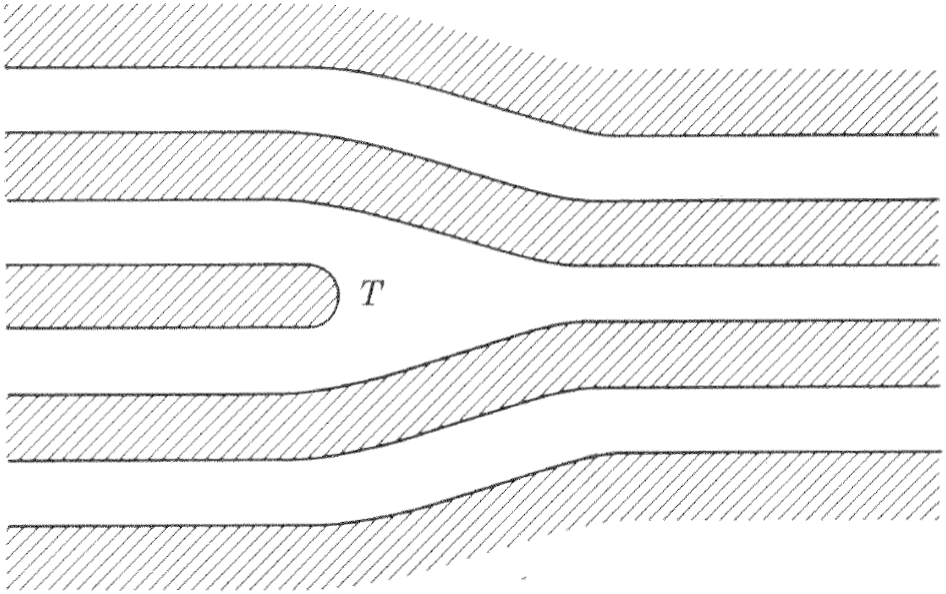

Fig. 6.16. Termination of lamellar (schematic)

The supercooling is calculated 1) at the intersection of a termination with the interface, and 2) at a position remote from terminations.

Assumptions: 1) Width of two lamellar ~ equal

2) Curvature ~ uniform and equal

3) Surface free energies of the two phases (α and β) ~ equal

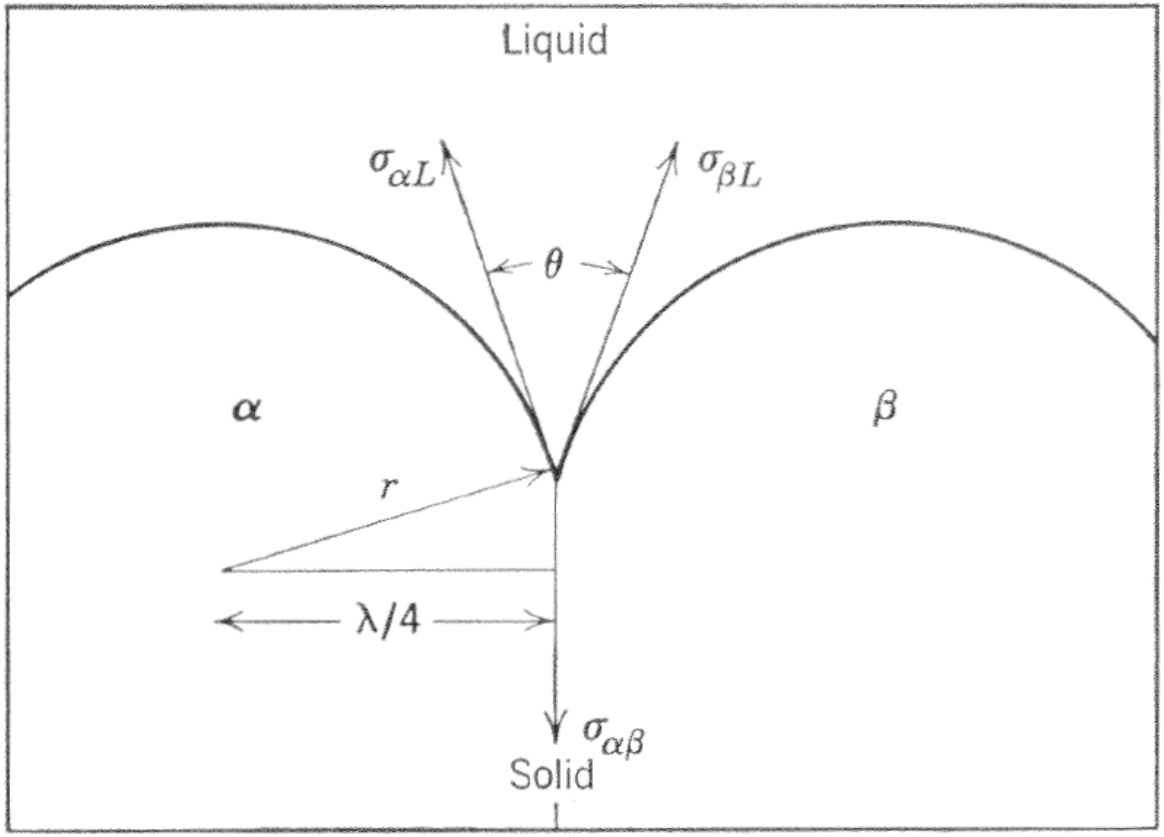

$$2\sigma_{\alpha L}\cos\frac{\theta}{2} = \sigma_{\alpha\beta}$$

$$\frac{\lambda}{4} = r\cos\frac{\theta}{2}$$

$$\cos\frac{\theta}{2} = \frac{\sigma_{\alpha\beta}}{2\sigma_{\alpha L}} = \frac{\lambda}{4r}$$

$$\frac{\sigma_{\alpha L}}{r} = \frac{2\sigma_{\alpha\beta}}{\lambda}$$

Fig. 6.17. Region of interface near the junction of two lamellae.

Diffusion of solute ahead of the interface

$$(C_\alpha{}^L - C_E) = [(1 - k_\alpha)C_E R\lambda]/8D$$

$$\Delta T_c = [(1 - k_\alpha)C_E R\lambda m_\alpha]/8D$$

m : slope of liquidus line
R : rate

Supercooling at curvature center

$$\Delta T_r = \frac{\sigma_{\alpha L} T_E}{Lr} \quad \text{but} \quad \frac{\sigma_{\alpha L}}{r} = \frac{2\sigma_{\alpha\beta} T_E}{L\lambda}$$

and therefore

$$\Delta T_r = \frac{2\sigma_{\alpha\beta} T_E}{L\lambda}$$

At termination point T, Curvature change (cylindrical → Spherical)

$$\Delta T_r = 4\sigma_{\alpha\beta} T_E / L\lambda$$

Amount of solute rejected by the half cylinder of the termination (assumed to be stable),

$$(1 - k_\alpha) C_E R (\pi/2) (\lambda^2/16)$$ **per unit time**

Amount of solute diffuses across the semicircular interphase boundary

$$(1 - k_\alpha) C_E R \frac{\pi}{2} \frac{\lambda^2}{16} = \frac{D(C_\alpha{}^L - C_E)\lambda/2}{\lambda/4} \pi \frac{\lambda}{4}$$

or

$$C_\alpha{}^L - C_E = \frac{(1 - k_\alpha) C_E R \lambda}{16D}$$

from which

$$\Delta T_c = \frac{m_\alpha (1 - k_\alpha) C_E R \lambda}{16D}$$

The sums of the two supercoolings are equated, giving

$$\lambda^2 R = \frac{32\sigma_{\alpha\beta} T_E D}{m_\alpha (1 - k_\alpha) C_E L}$$

from which $\lambda^2 R$ is a constant, or, $\lambda \propto R^{-1/2}$.

$$v_0 \lambda_0^2 = k_3$$

$$\frac{v_0}{(\Delta T_0)^2} = k_4$$

5) Lamellar growth: experimental

$$v_0 \lambda_0^2 = k_3 \quad \text{(constant)}$$

$$\frac{v_0}{(\Delta T_0)^2} = k_4$$

Al-Zn, Al-Cu, Al-Zn, Pb-Sn, Pb-Cd
good agreement

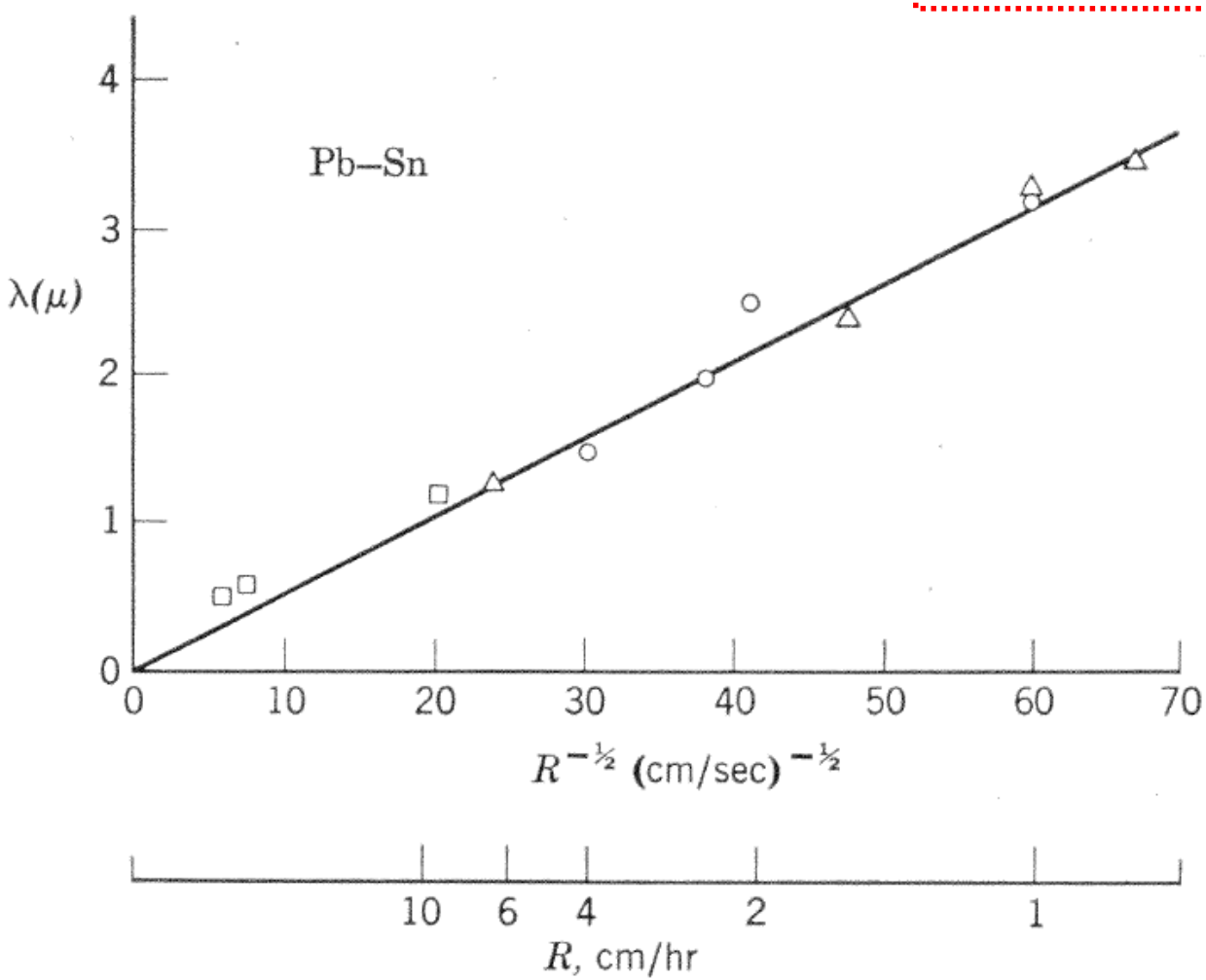

Fig. 6.18. Relationship between interlamellar spacing and growth rate for the lead–tin eutectic.

5) Lamellar growth: experimental

Al-Zn, Al-Cu, Al-Zn, Pb-Sn, Pb-Cd
good agreement

$$\nu_0 \lambda_0^2 = k_3 \text{ (constant)}$$

$$\frac{\nu_0}{(\Delta T_0)^2} = k_4$$

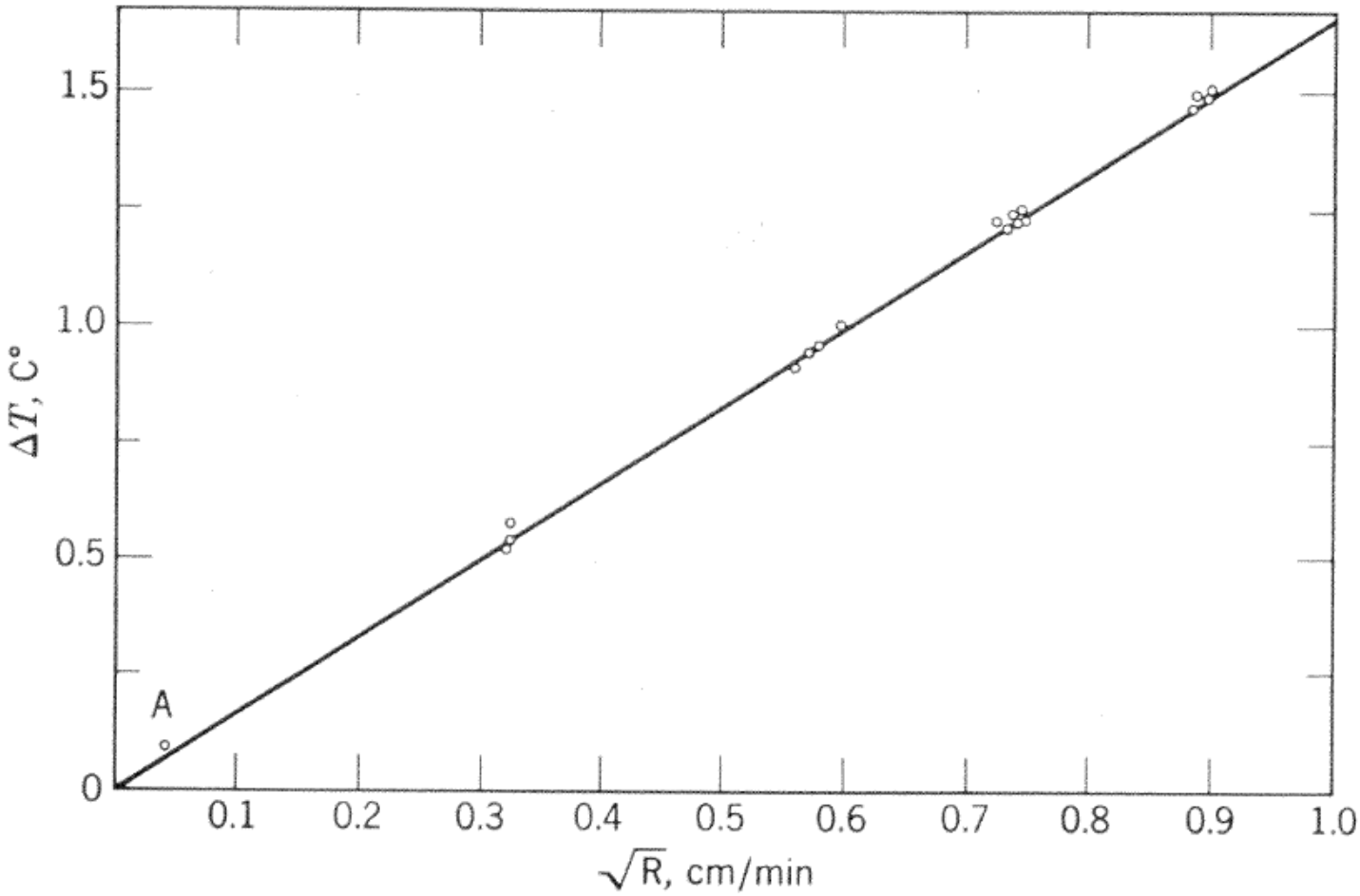

Fig. 6.19. Supercooling of eutectic interface as a function of growth rate (lead–tin).

6) Degenerate eutectic structure

Pure eutectic (lamellar type) ~ a very wide range of solidification rate

→ structure degenerate at very slow rates of solidification (less than 1cm/hr)

*** Degenerate structure:**
resemble the beginning of the spheroidization process that occurs during prolonged annealing

→ But, the degenerate structure is formed during, and not after, solidification.

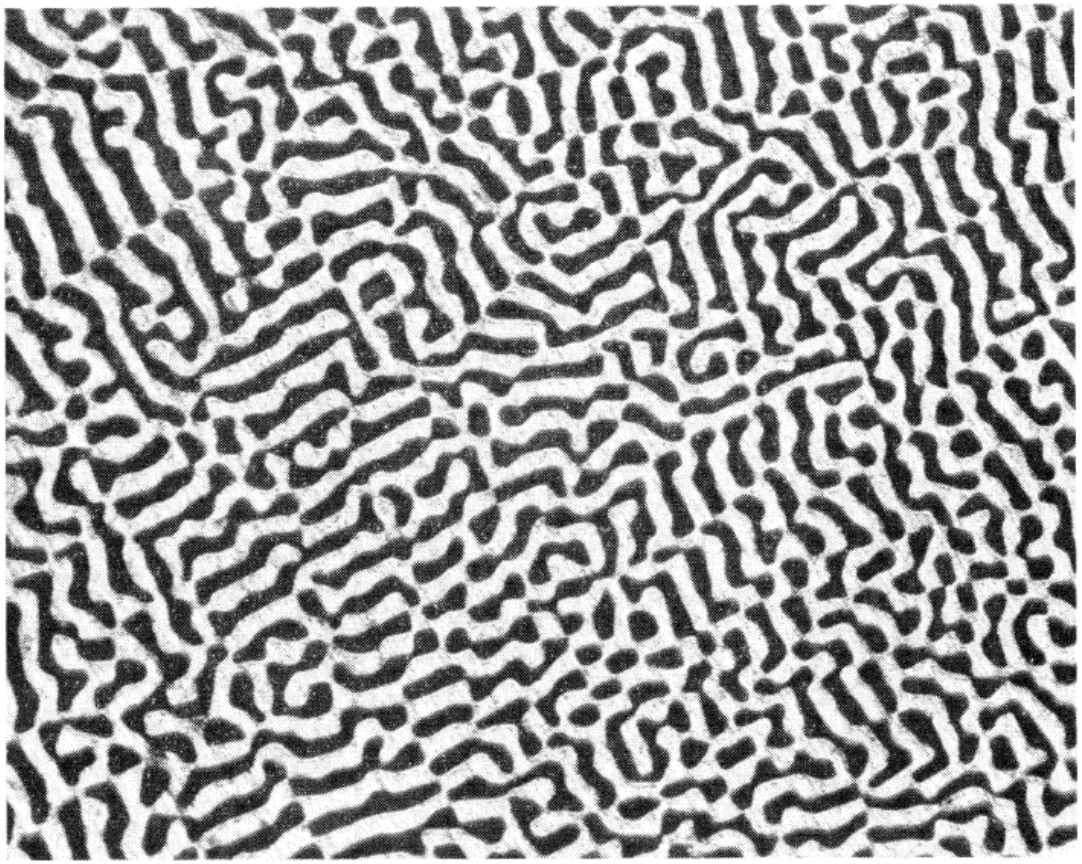

Fig. 6.20. Degenerate eutectic structure in CuAl2–Al eutectic at 0.8 cm/hr (X500).

7) Modification of Eutectics

Two degenerate forms of the lamellar structure by impurities

→ (a) Colony structure and (b) Rod structure

(a) Colony structure

: a cellular structure superimposed on the lamellar eutectic structure

*** An impurity or an excess of one constituent, would diffuse much farther ahead of the interface than would be required for transverse interlamellar diffusion**

→ The long range diffusion sets up constitutional supercooling → Cell formation and the resulting transverse diffusion of the impurity

→ if purity of the eutectic were sufficiently high, the colony structure are eliminated (regular lamellar structure is produced)

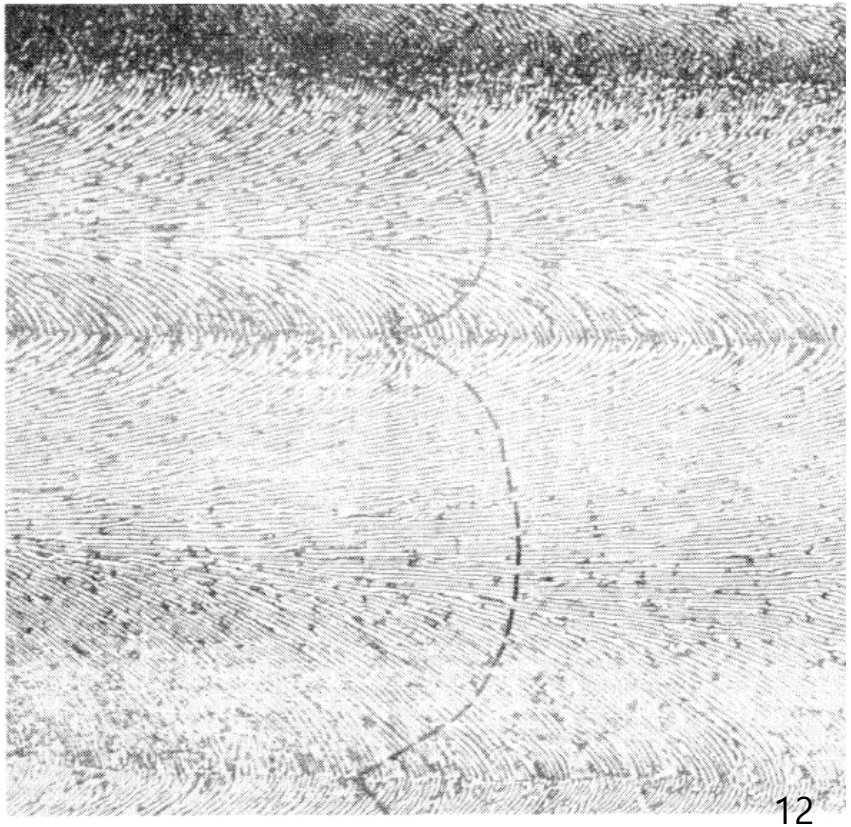

Fig. 6.21. Longitudinal section of impure $CuAl_2$–Al eutectic alloy. Broken line indicates shape of interface during growth.

A planar eutectic front is not always stable.

Binary eutectic alloys contains impurities or other alloying elements ➡ **Form a cellular morphology**
analogous to single phase solidification
Restrict in a sufficiently high temp. gradient.

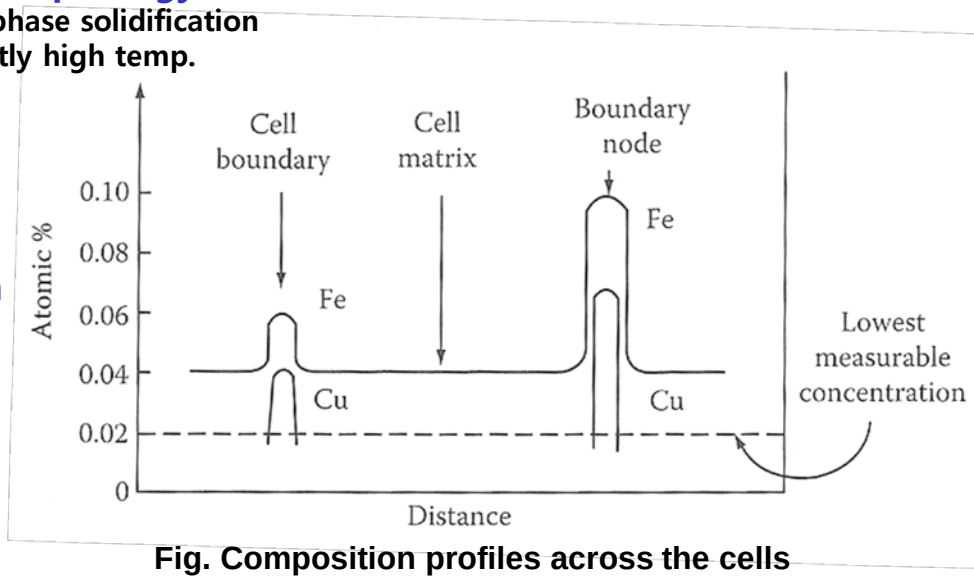

Fig. Composition profiles across the cells

➡ **The solidification direction changes as the cell walls are approached and the lamellar or rod structure fans out and may even change to an irregular structure.**

➡ **Impurity elements (here, mainly copper) concentrate at the cell walls.**

* Total Undercooling $\Delta T_0 = \Delta T_r + \Delta T_D$

Undercooling required to overcome the interfacial curvature effects

Undercooling required to give a sufficient composition difference to drive the diffusion

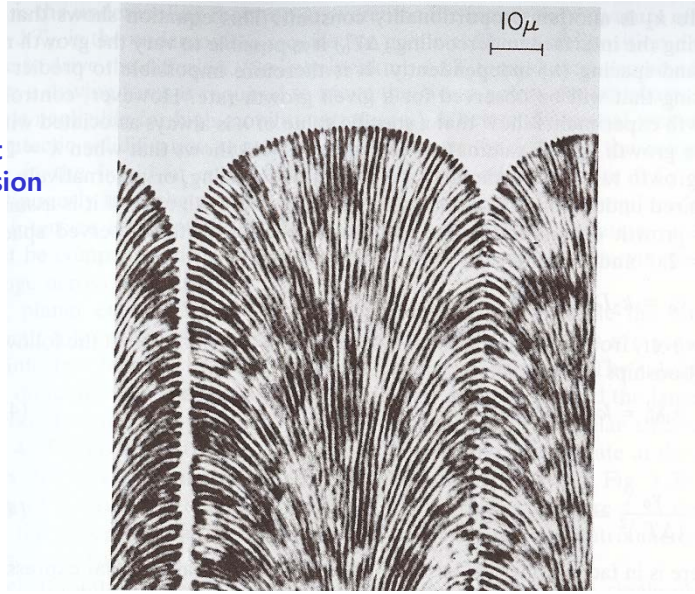

Strictly speaking,

ΔT_i term should be added — but, negligible for high mobility interfaces

Driving force for atom migration across the interfaces

$\Delta T_D \rightarrow$ Vary continuously from the middle of the α to the middle of the β lamellae

$\Delta T_0 = const$ ← Interface is essentially isothermal.

$\Delta T_D \rightarrow \Delta T_r$ The interface curvature will change across the interface.

Should be compensated

(b) Rod structure

: Impurity has sufficiently different distribution coefficients for the two solid phases

*** When the two distribution coefficient are very different, the lamellae of one phase should grow into the liquid ahead of the other, and the lamellae of the lagging phase then break up into very small cells, separated by the other phase.**

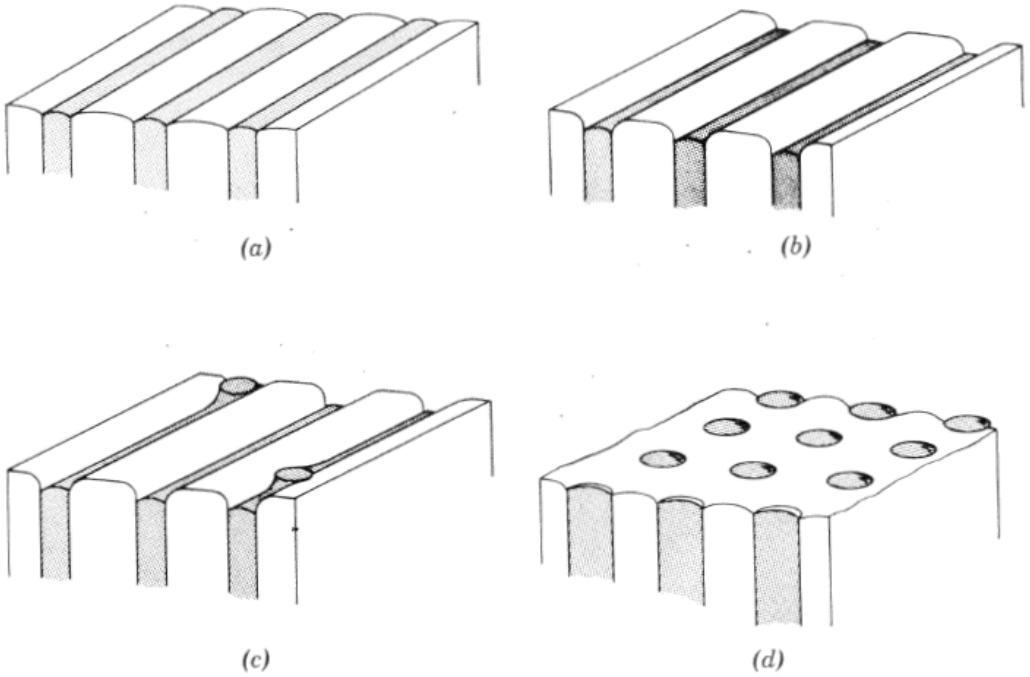

Fig. 6.22. Origin of "rod-type" eutectic structure (schematic).

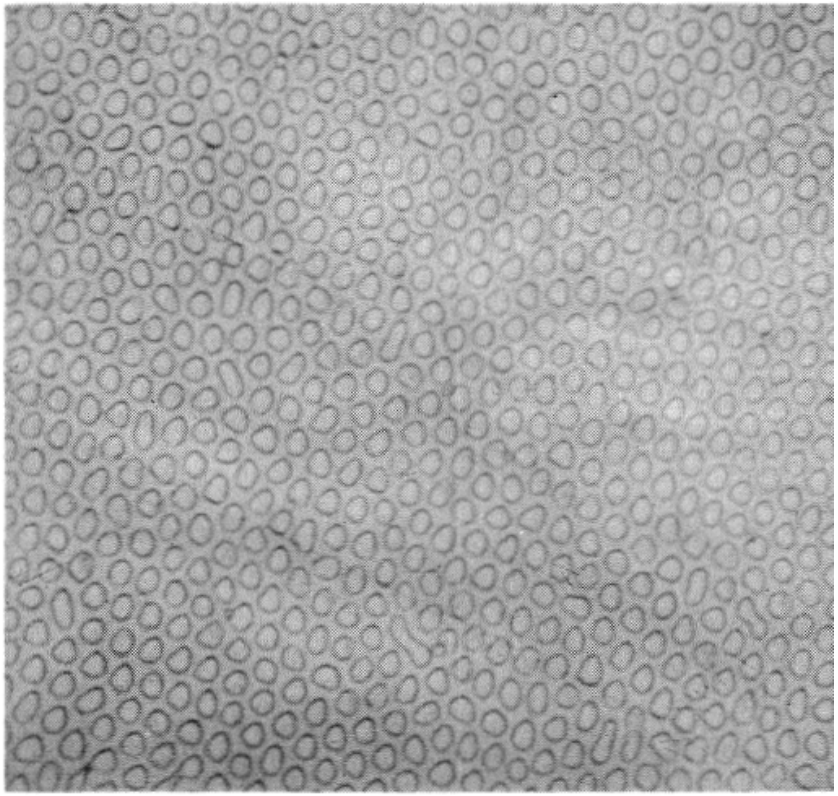

Fig. 6.23. Cross section of "rod-type" eutectic structure.

(C) Intermediate structure: Middle= lamellar structure/ edge = rod-type colony

: **This is caused by an impurity which when present at a low concentration, has nearly equal distribution coefficient for the two solid phases, but which has increasingly differing distribution coefficients as its concentration increases.**

*** Middle part of Cell**

: relatively low concentration of impurity & similar distribution coefficients

→ **Lamellar structure**

*** Edge of cell (near wall)**

: relatively high concentration of impurity & increasing differing distribution coefficients

→ **Rod-type structure**

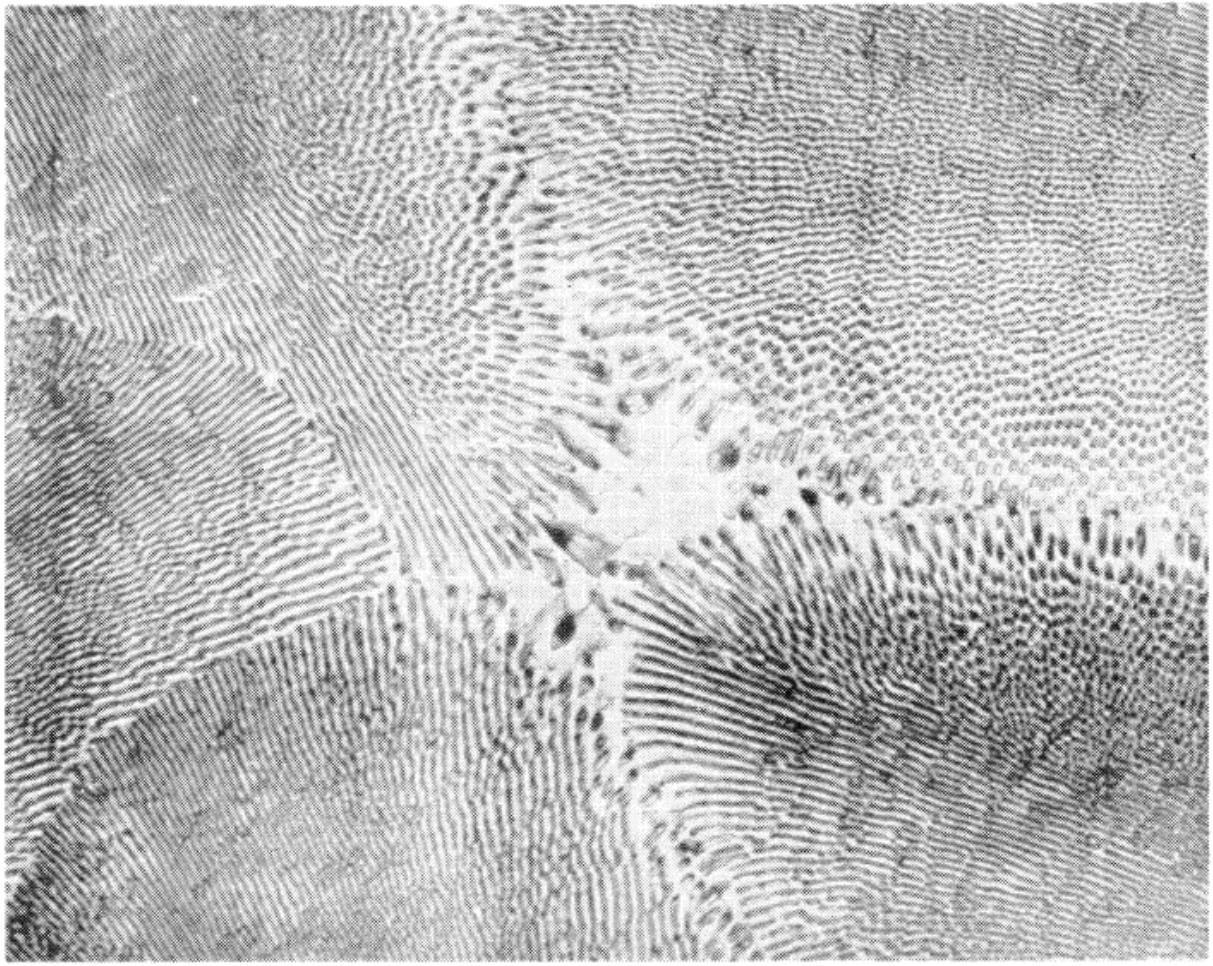

Fig. 6.24. "Mixed lamellar and rod structure" (Pb–Cd eutectic alloy with 0.1% Sn)

(d) Discontinuous eutectic structure

In lamellar type & degenerate form, each phase grows continuously
→ does not required repeated nucleation.

"Discontinuous eutectic" : required renucleate repeatedly due to "strong anisotropy" of growth characteristics of one of the phases

a) Case I: both phases renucleate repeatedly due to the termination of growth of crystals

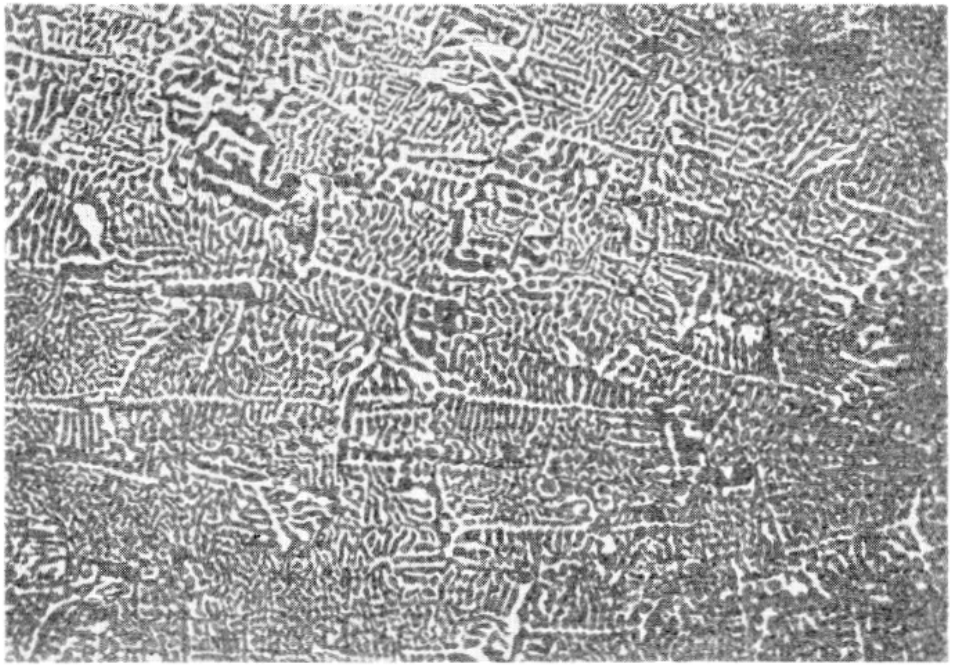

Fig. 6.25. "Chinese script" structure in Bi-Sn eutectic alloy

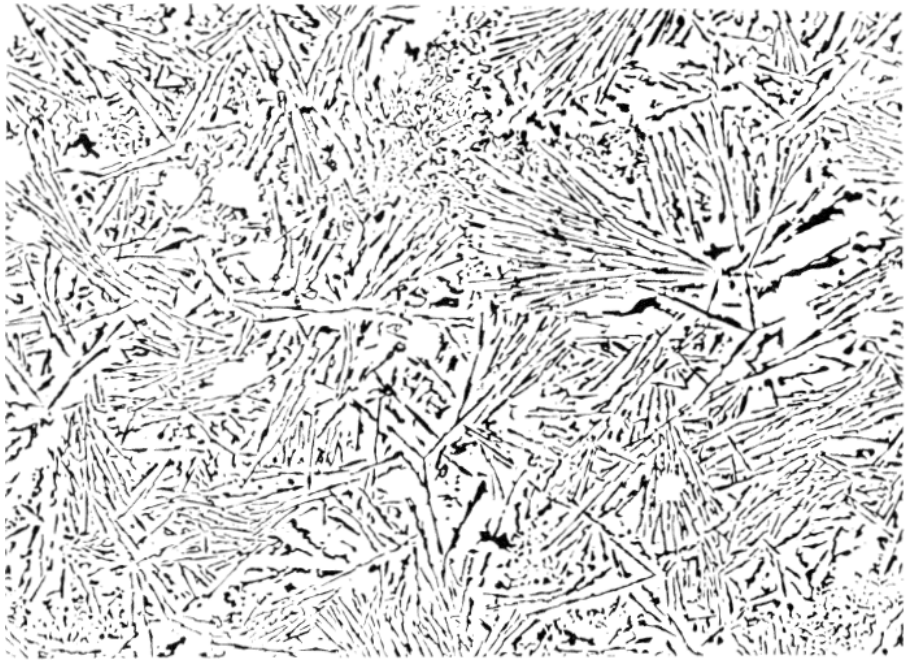

Fig. 6.26. Microstructure of Al-Si eutectic alloy.

(d) Discontinuous eutectic structure

: required renucleate repeatedly due to "strong anisotropy" of growth characteristics

a) Case I: both phases renucleate repeatedly due to the termination of growth of crystals

*** Typical discontinuous eutectic type growth mechanism (Figure 6.26)**

- Random nucleation and growth independent with growth interface

- I_1: three Si phases (A, B, C) growth
B= block of growth of C
A & B distance increase
I_2 : Nucleation and growth of D

- Chinese script (Fig. 6.25) type has not been investigated sufficiently.

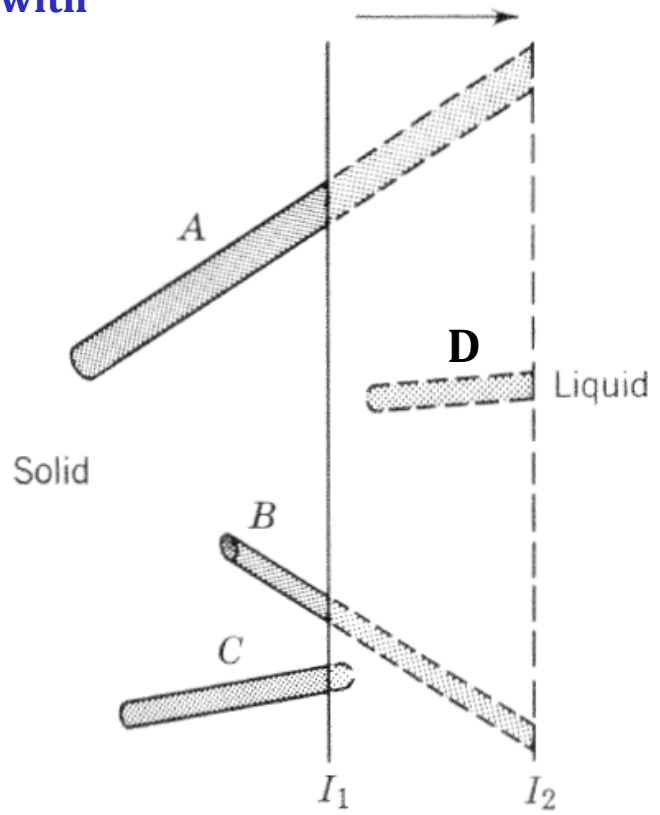

Fig. 6.27. Growth of a discontinuous eutectic (schematic), showing two positions of the interface (I_1 and I_2).

(d) Discontinuous eutectic structure

b) "Spiral type의 discontinuous eutectic" **- Al-Th & Zn-Mg alloys**

: one or both of the phases → <u>anisotropic in growth rate</u>

→ α phase grows faster than the β phase in one direction and more slowly in the other (unusual structure in Fig. 6.30).

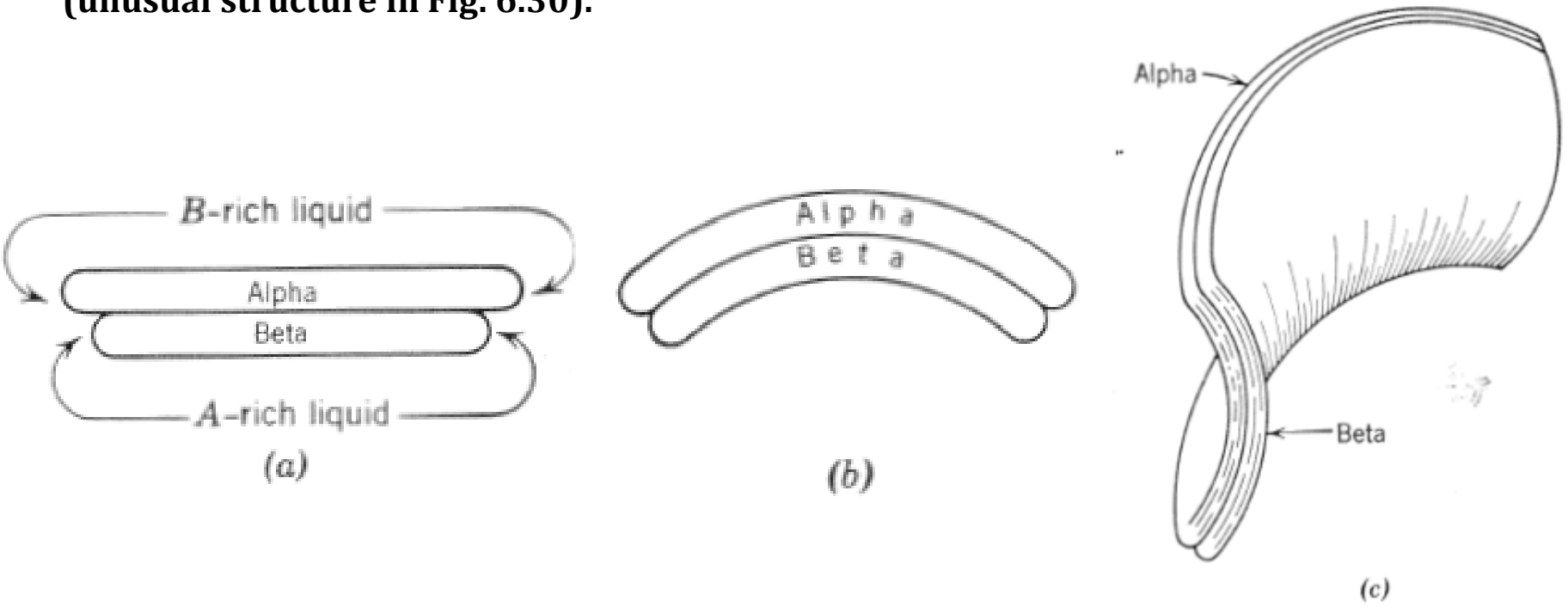

Fig. 6.30. Origin of spiral eutectic (schematic).

(d) Discontinuous eutectic structure

b) "Spiral type의 discontinuous eutectic" - Al-Th & Zn-Mg alloys

: one or both of the phases → anisotropic in growth rate

*** If the two edges of the β phase do not form a closed ring, but overlap, then a spiral will be formed in that plane, and the complete structure will develop into a double conical spiral as shown in Fig. 6.29.**

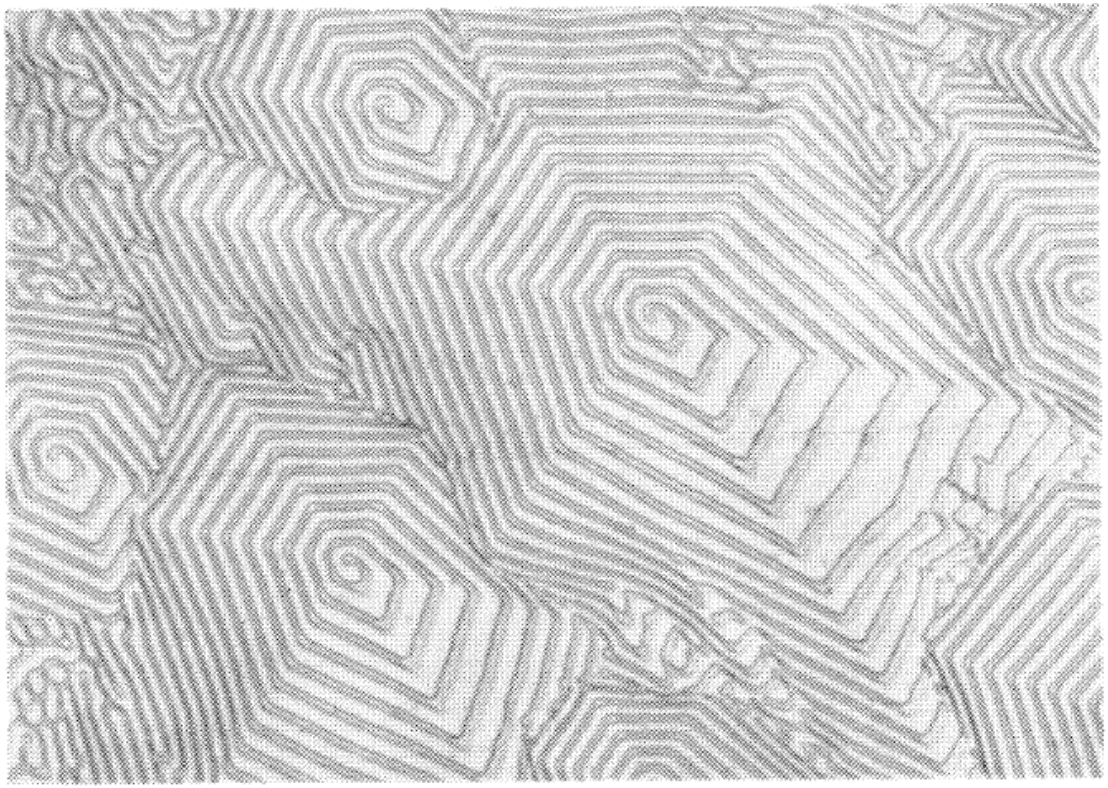

Fig. 6.28. Spiral eutectic structure in Zn–Mg alloy.

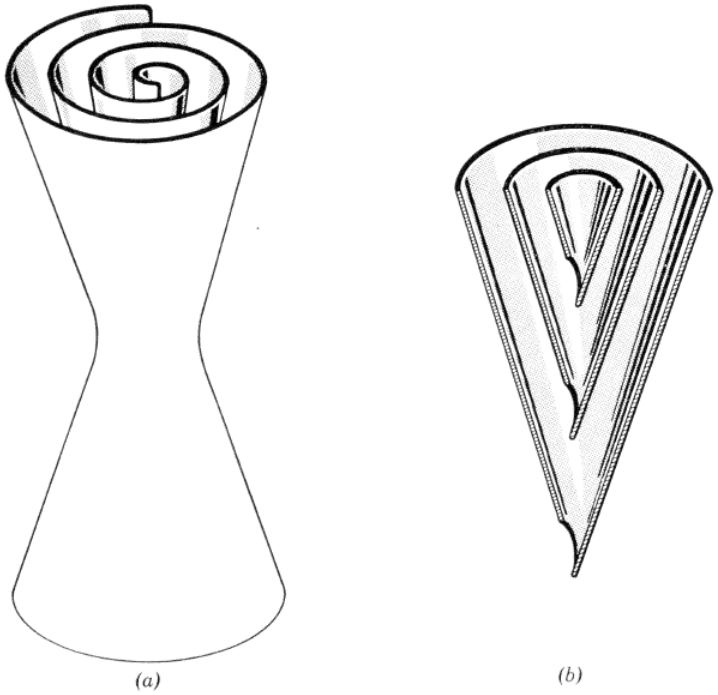

Fig. 6.29. Detailed structure of the spiral eutectic (schematic).

(e) Special cases of the modification of eutectics

Ex) Microstructure of Al-Si eutectic could be modified by the minor addition of solutes:

① Addition of 0.01 % Sodium

Needle or plate type Si morphology → very smaller, more spherical Si particles

② Rapid Cooling → very smaller, more spherical Si particles

*** An explanation for these phenomena**

→ the modified structure is formed at a temp. a few degrees below the normal T_e.

① Modifier changes the surface tension relationships (due to lower latent heat and higher thermal conductivity of Al) → very smaller, more spherical Si particles

② Rapid quenching →

due to thermal difference

→ Large supercooling

a. decrease of Si precipitation (follows EA line)

b. decrease of r* of Si and constantly re-nucleating Si

→ very smaller, more spherical Si particles

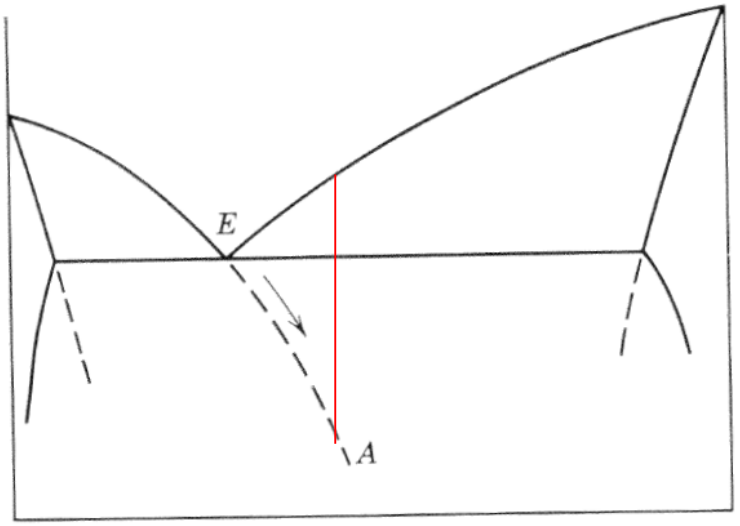

Fig. 6.31. Supercooling of eutectic in the absence of the second phase.

8) Non-eutectic composition

Solidification of C_0 liquid

① complete mixing: Primary α $C_s \rightarrow C_T$

Liquid 조성 $C_0 \rightarrow E$

② less complete mixing: primary solidification

Depending on undercooling: Cellular →

Cellular-dendritic → New crystal nuclei

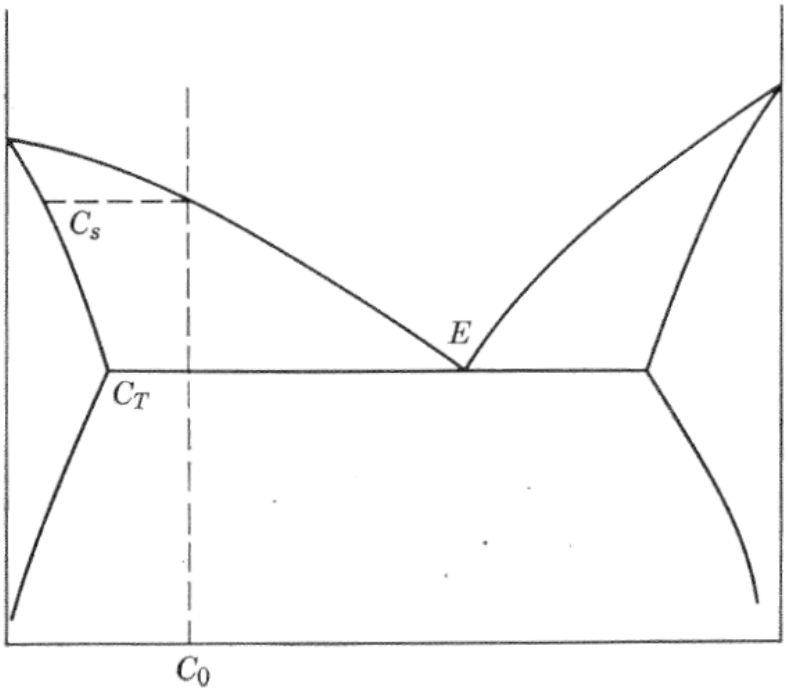

Fig. 6.32. Soldification of a eutectic system at a non-eutectic composition.

In real cases, the terminal transient liquid is far richer in solute than would be predicted from the equilibrium diagram, and it is therefore difficult to avoid the formation of some eutectic if the relevant liquid line terminates at a eutectic point.

* Off-eutectic Solidification

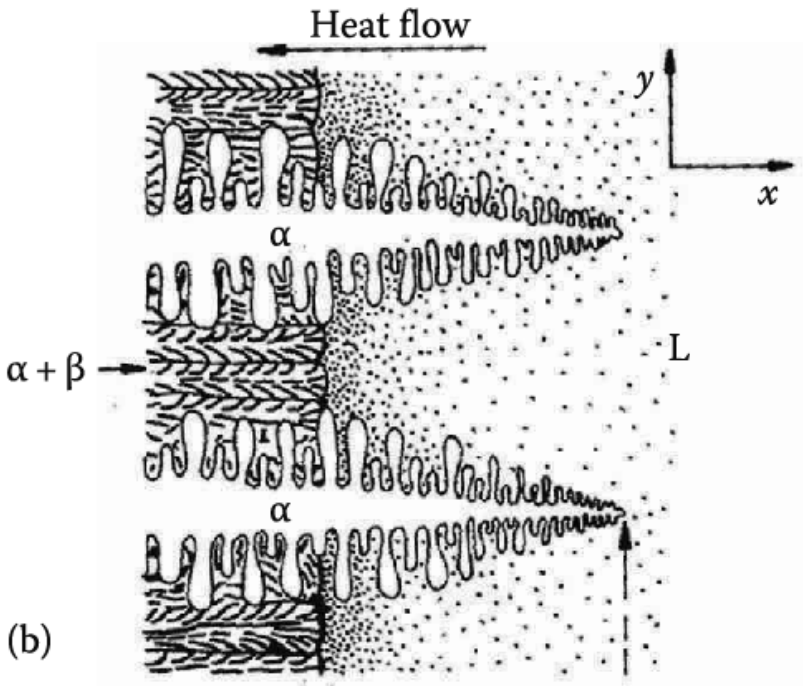

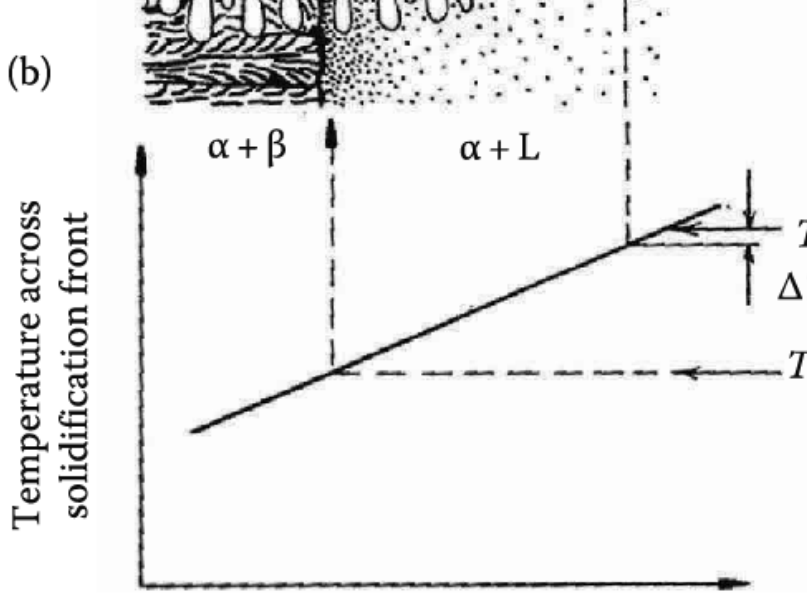

primary α + eutectic lamellar

- **Primary α dendrites form at T_1. Rejected solute increases X_L to X_E; eutectic solidification follows.**
- **Coring: primary α (low solute) at T_1 and the eutectic (high solute) at T_E.**

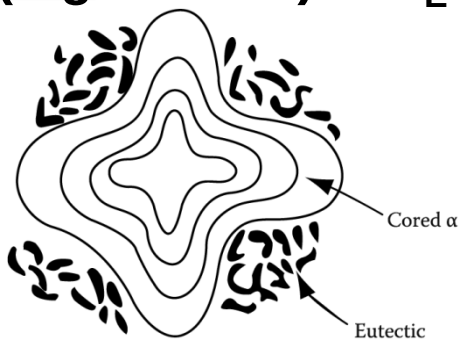

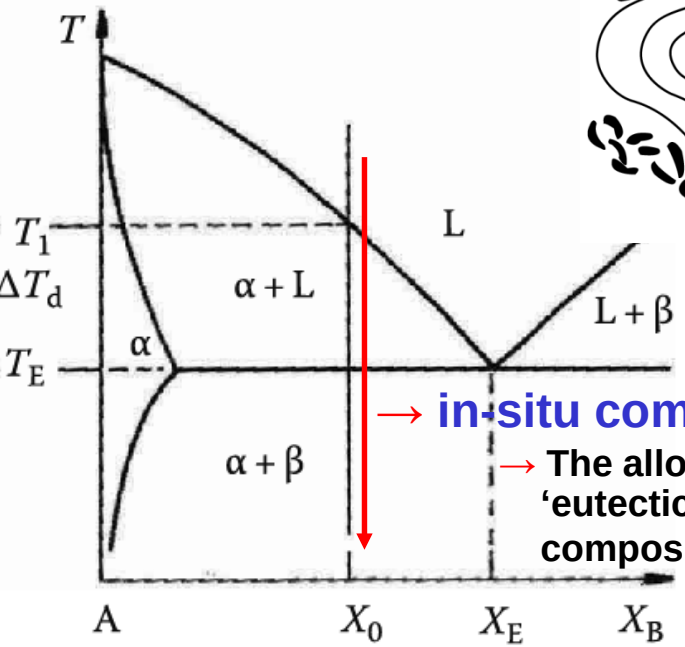

→ **in-situ composite materials**

→ **The alloy solidifies as 100% 'eutectic' with an overall composition X_0 instead of X_E.**

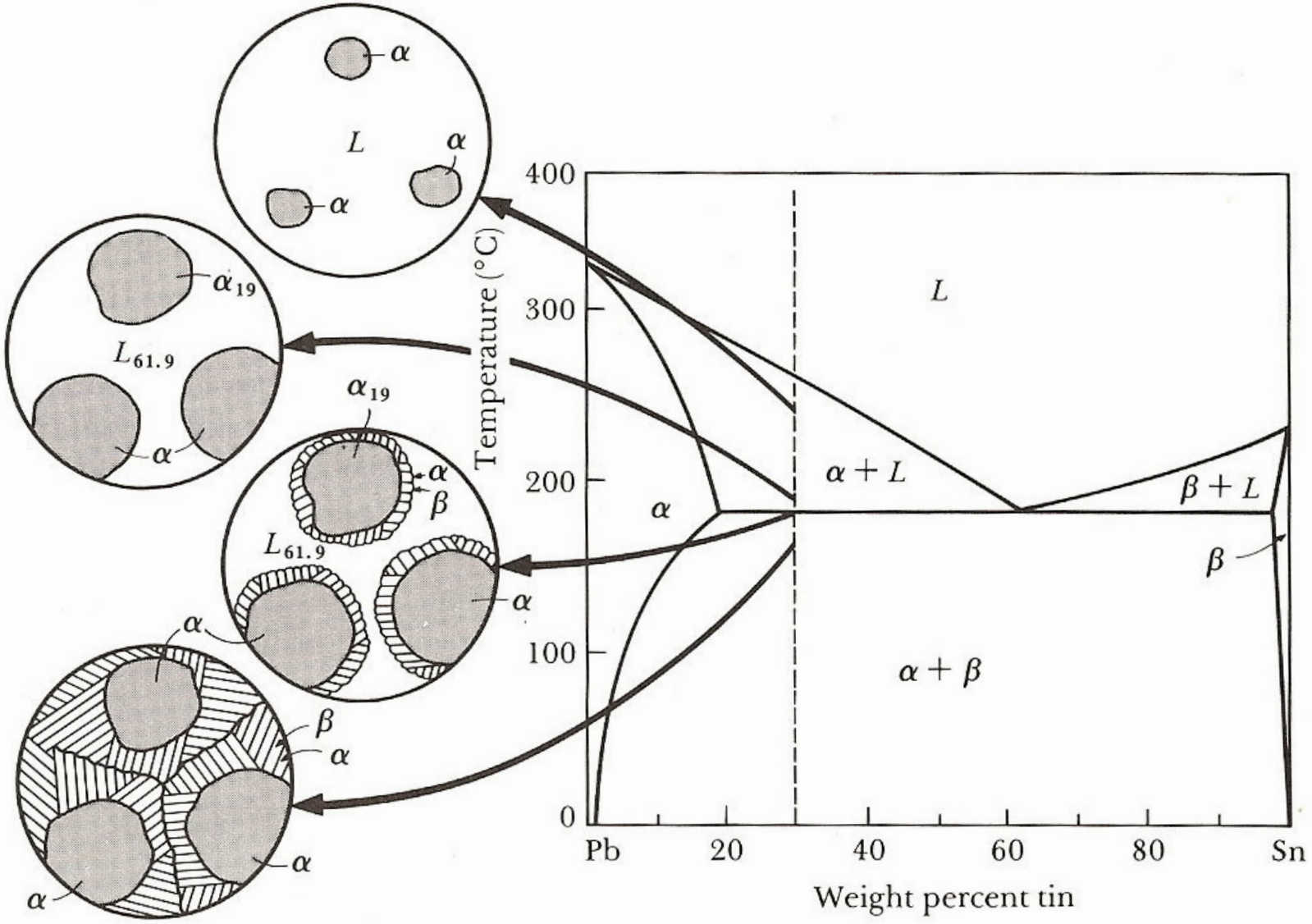

FIGURE 10-12 The solidification and microstructure of a hypoeutectic alloy (Pb-30% Sn).

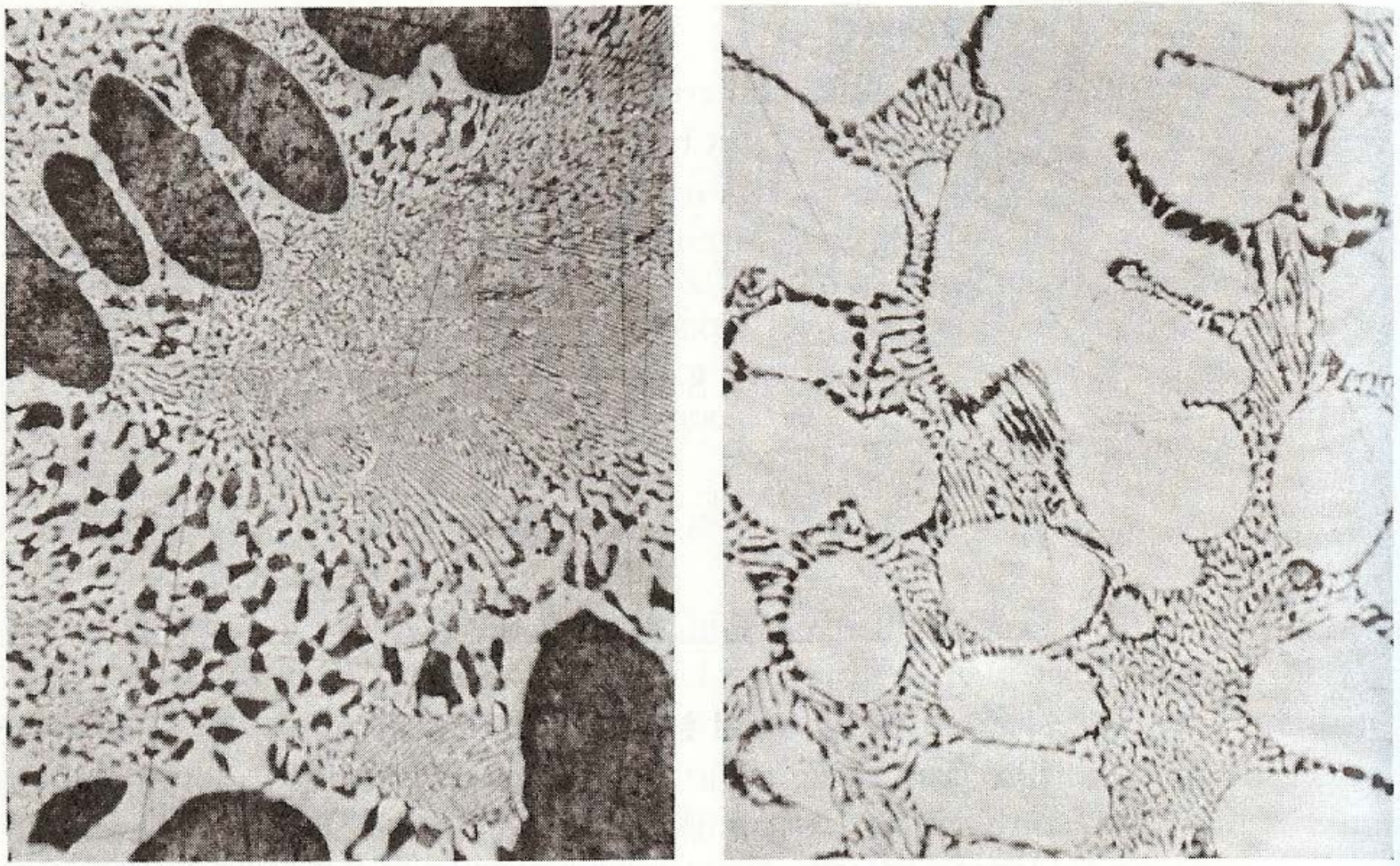

(a) (b)

FIGURE 10-13 (a) A hypoeutectic lead-tin alloy. (b) A hypereutectic lead-tin alloy. The dark constituent is the lead-rich solid α, the light constituent is the tin-rich solid β, and the fine plate structure is the eutectic ($\times$ 400).

9) Gravity segregation of eutectic

* Uranium-Al eutectic region: “Cycled” up and down of T_E

→ marked segregation: crucible bottom_U concentration↑/ top: Al concentration↑

→ Degree of Segregation : depending on # of Cycles

Ex) Al-13.3 wt% U → 168 cycles → bottom 45.4%/ top only 2.2%

: The segregation is in fact a result of the motion of the liquid enriched with solute during solidification and of the purer liquid formed by melting the separated phases during melting part of the cycle.

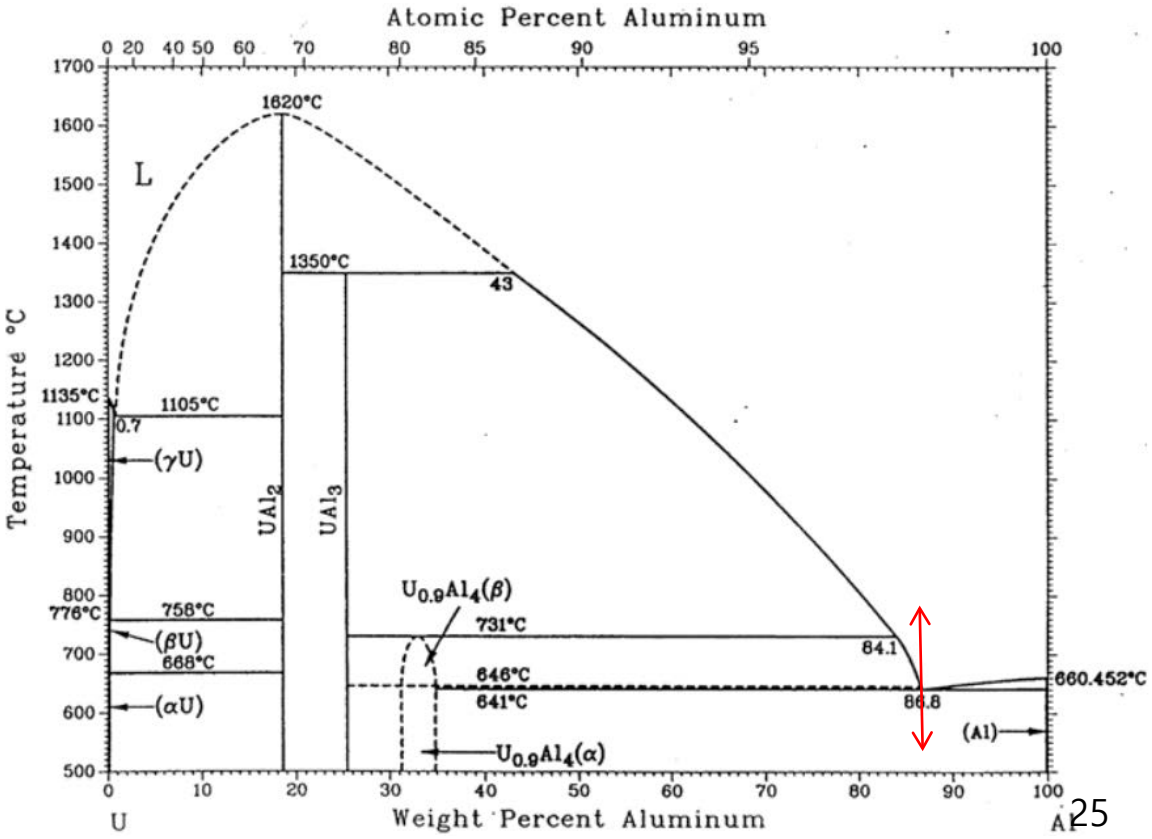

10) Divorced eutectic

- The primary phase continues to solidify past the eutectic point (along the line EA) of Fig. 6.31 until either the whole of the liquid has solidified or the other phase nucleated and forms a layer, which is some times dendritic, separating the two layers of the primary phase.

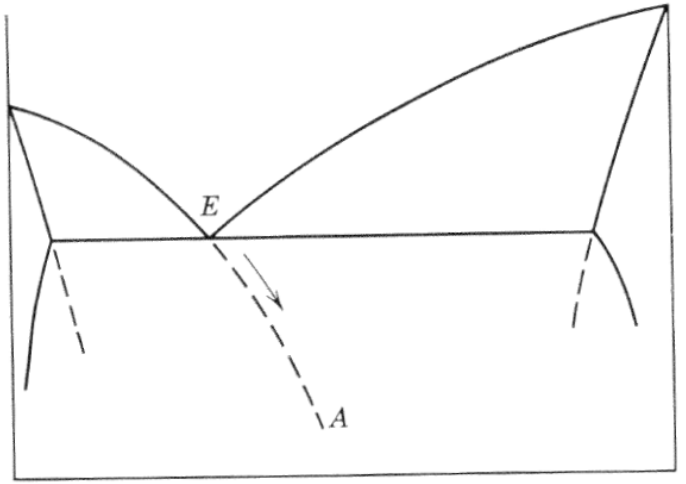

Fig. 6.31. Supercooling of eutectic in the absence of the second phase.

- One of the phases requires considerable supercooling for nucleation.

- "Divorced eutectic" is used to denote eutectic structures in which one phase is <u>either absent or present in massive form.</u>

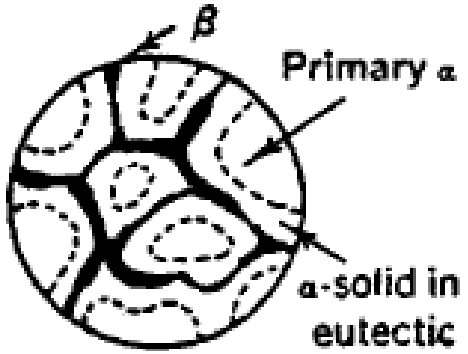

- **Massive Transformation**
  : The original phase decomposes into one or more new phases which have the same composition as the parent phase, but different crystal structures.

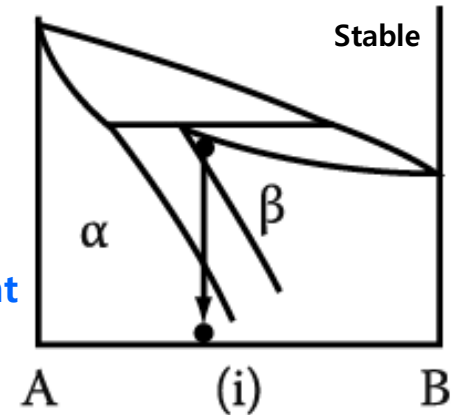

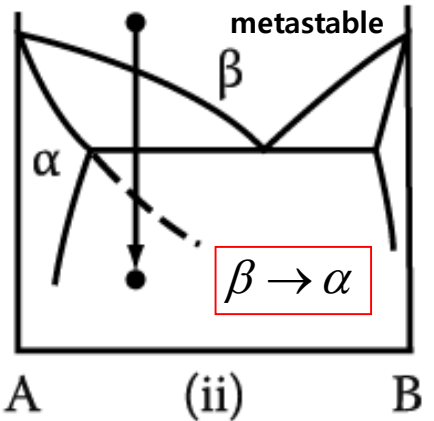

11) Ternary eutectic: very little work has been reported

* lamellar form, alternating three phases in ternary eutectic of Pb-Sn-Cd

: This arrangement is the one which would provide the shortest possible diffusion path for a given total area of interphase boundary, since each phase is adjacent to both of the other two phases.

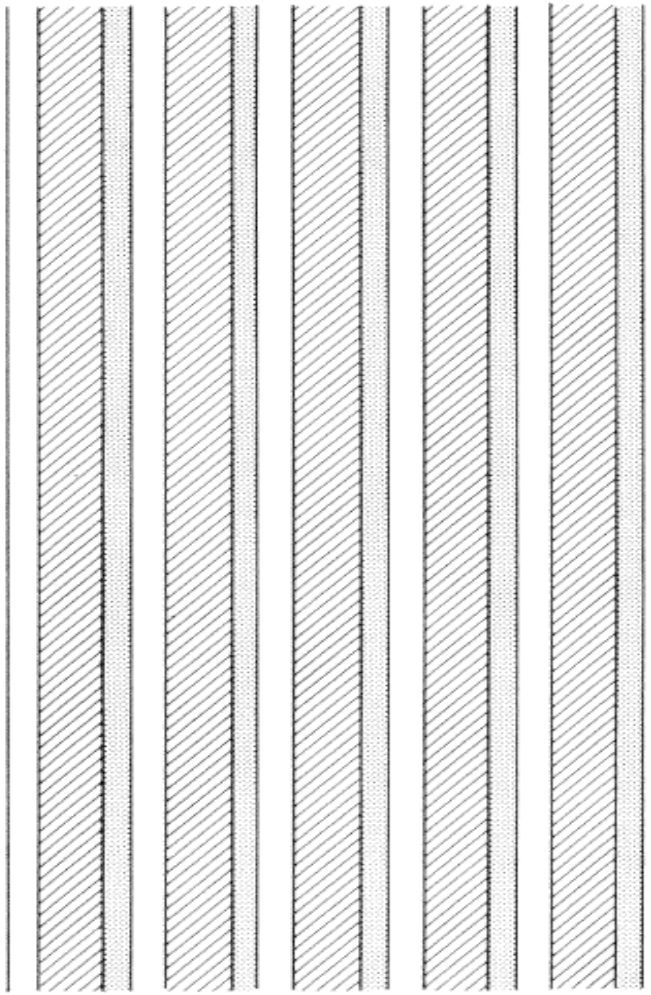

Fig. 6.34. Lamellar ternary eutectic.

- **IH _ Summary of recently reported paper for Quar-ternary or higher eutectic (within 3 pages of PPT)**

Ferrous Alloys

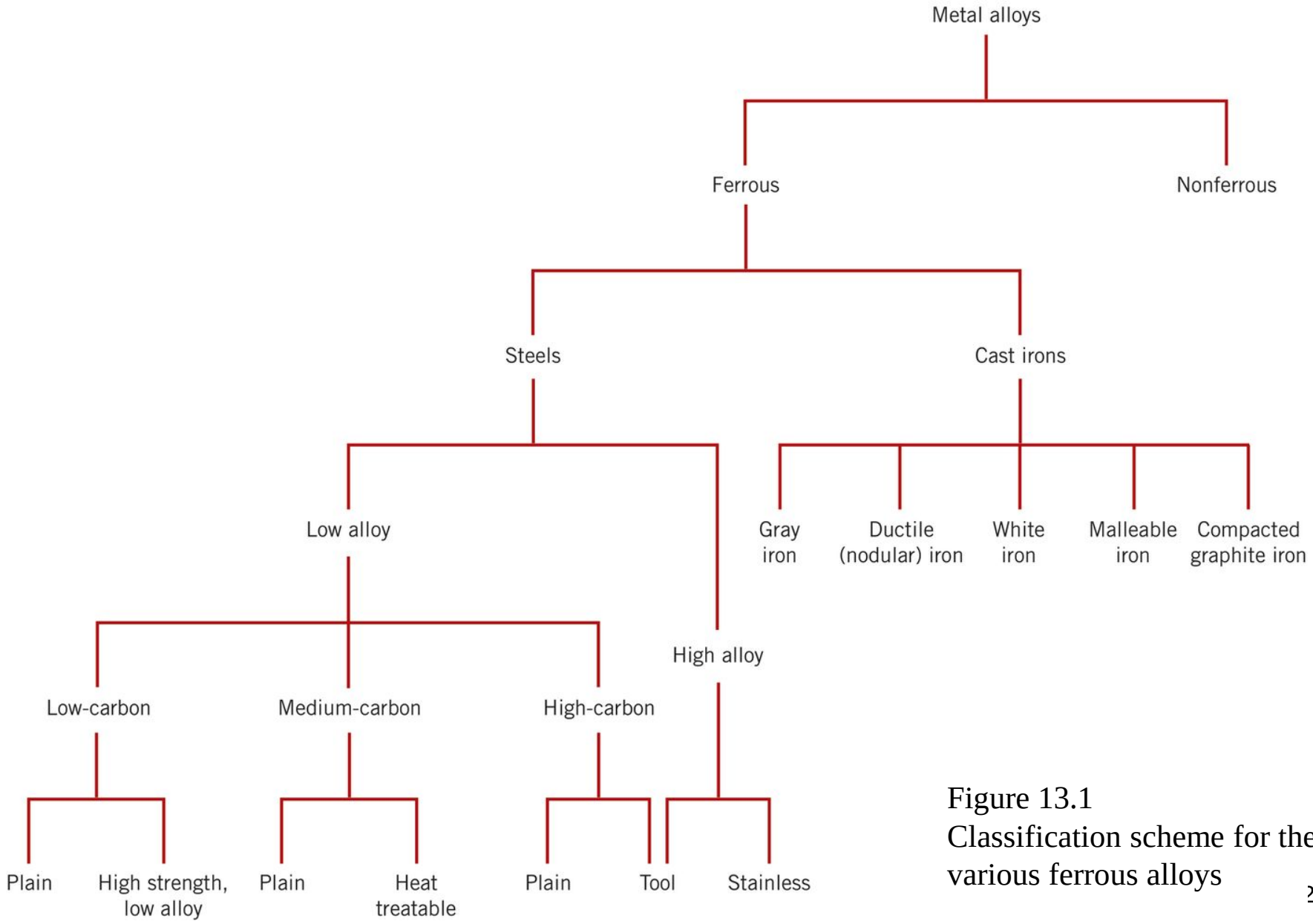

Figure 13.1
Classification scheme for the various ferrous alloys

Steels

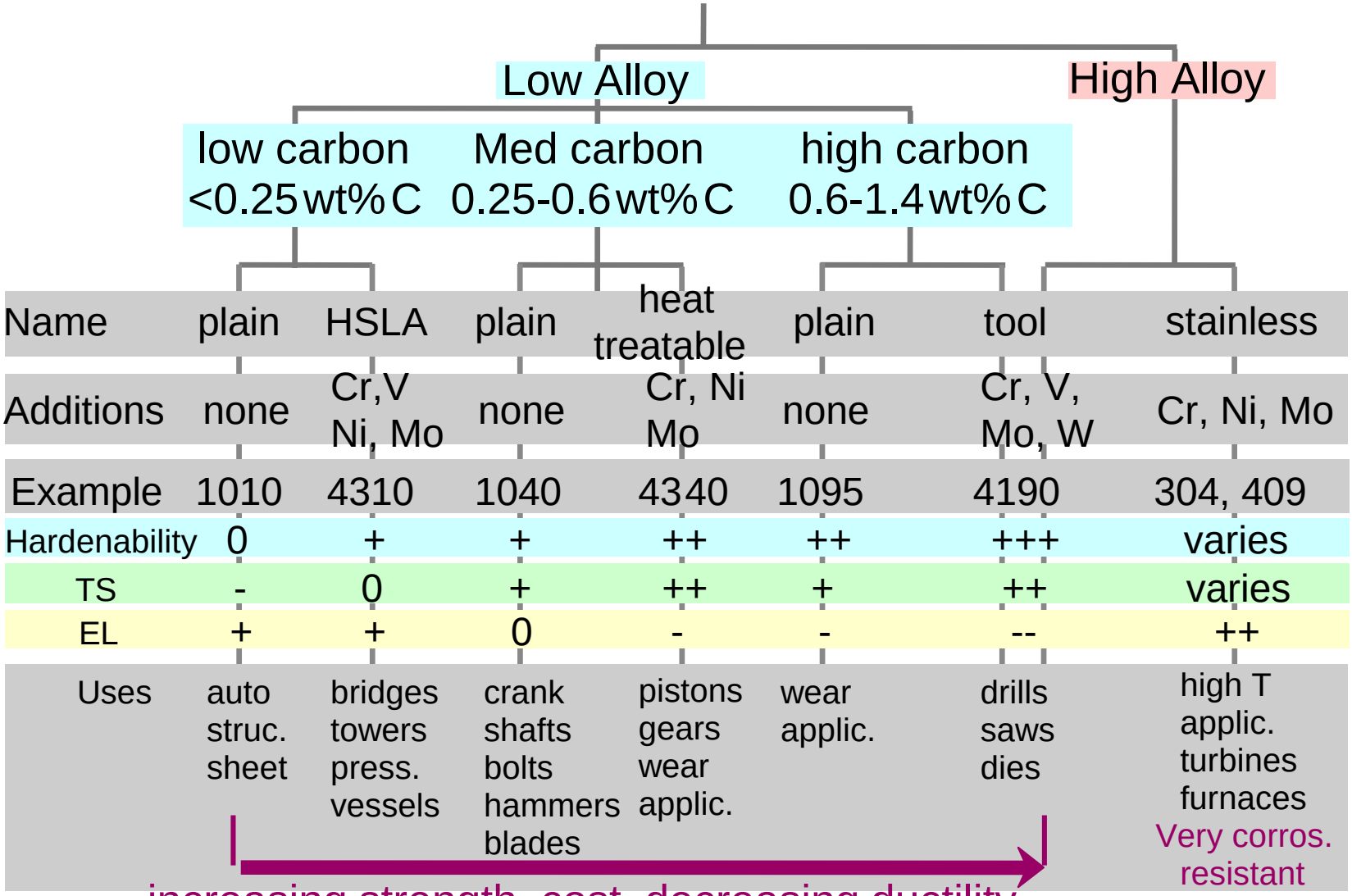

Based on data provided in Tables 13.1(b), 14.4(b), 13.3, and 13.4, *Callister & Rethwisch 9e.*

Cast Irons

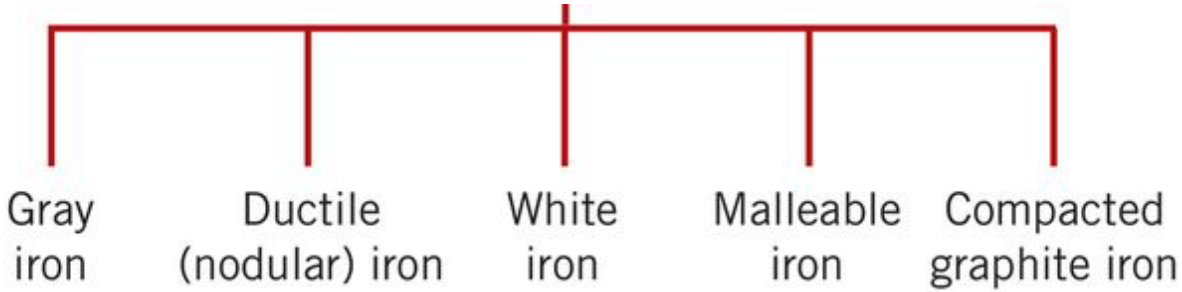

- Ferrous alloys with > 2.1 wt% C
  - more commonly 3 - 4.5 wt% C
- Low melting – relatively easy to cast
- Generally brittle
- Cementite decomposes to ferrite + graphite

  $Fe_3C \rightarrow 3\ Fe\ (\alpha) + C\ (graphite)$
  - generally a slow process

* Two eutectic system: Fe-graphite & Fe-Fe_3C

: If there is no other additive element, the Fe-graphite system is stable & Fe-Fe_3C (cementite) eutectic is formed by rapid cooling of liquid phase

* Classification of Cast Iron is possible depending on the type of Carbon.

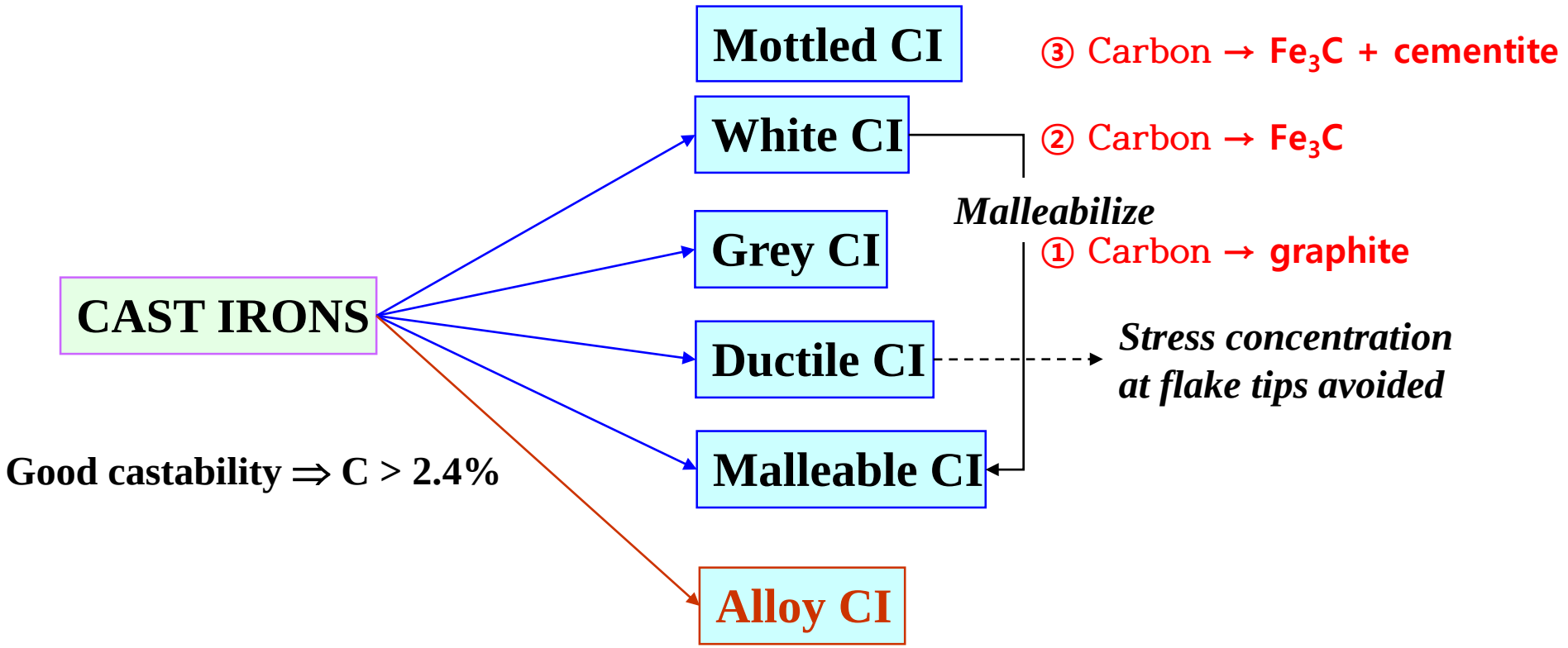

12) Cast Iron: Fe-C alloy (1.7 ≦ c ≦ 4.5%)

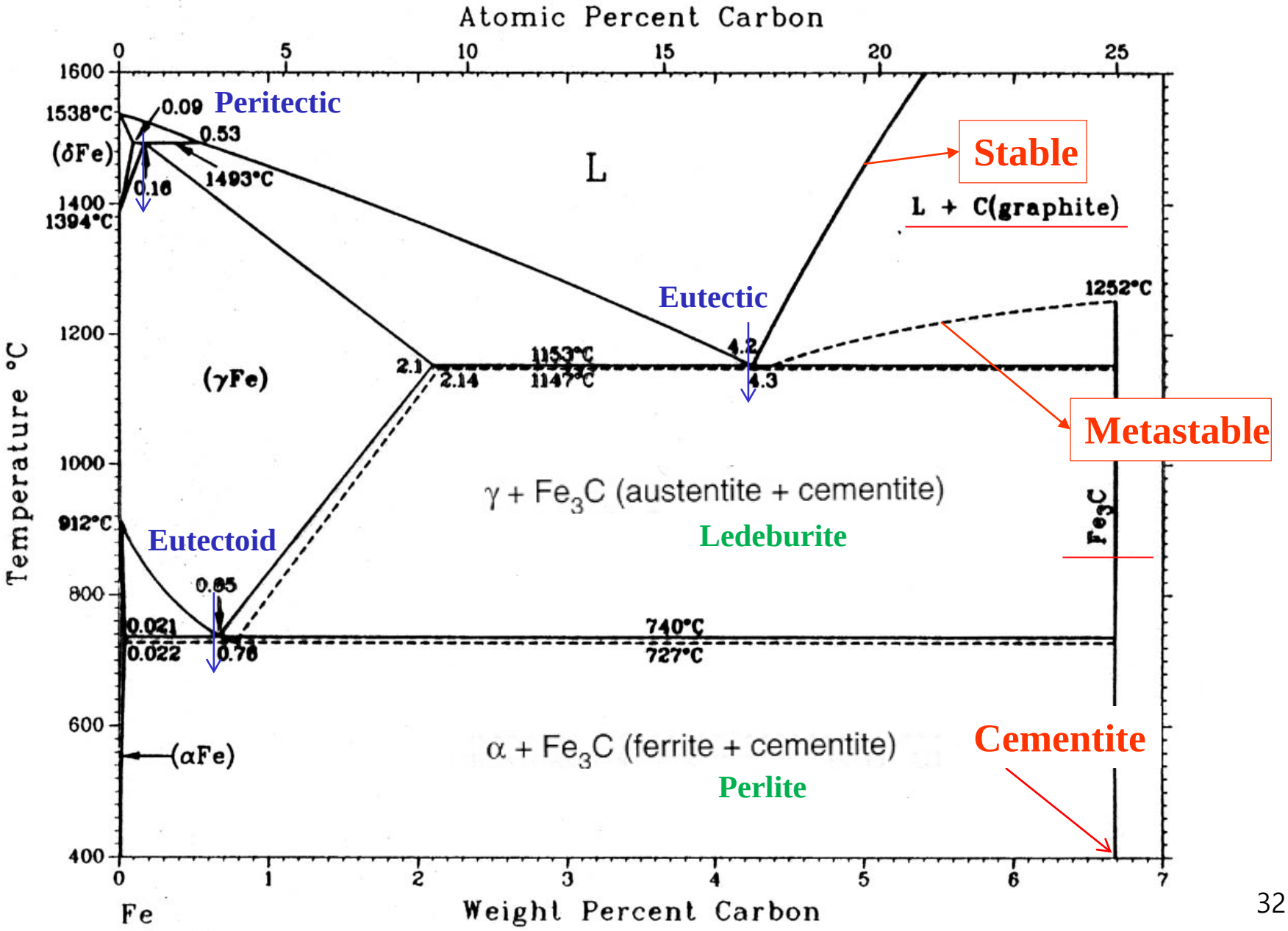

* Fe-Fe_3C eutectic temp (6°C) < Fe-graphite eutectic temp.

* If solidification proceeds at interface temperature above the cementite eutectic temperature,
  Graphite eutectic formation

→ Gray cast Iron

* If the solidification proceed below Cementite eutectic temperature due to lower the liquidus temperature through fast quenching and a suitable nucleation agent to form an over-solute layer,

→ White cast Iron

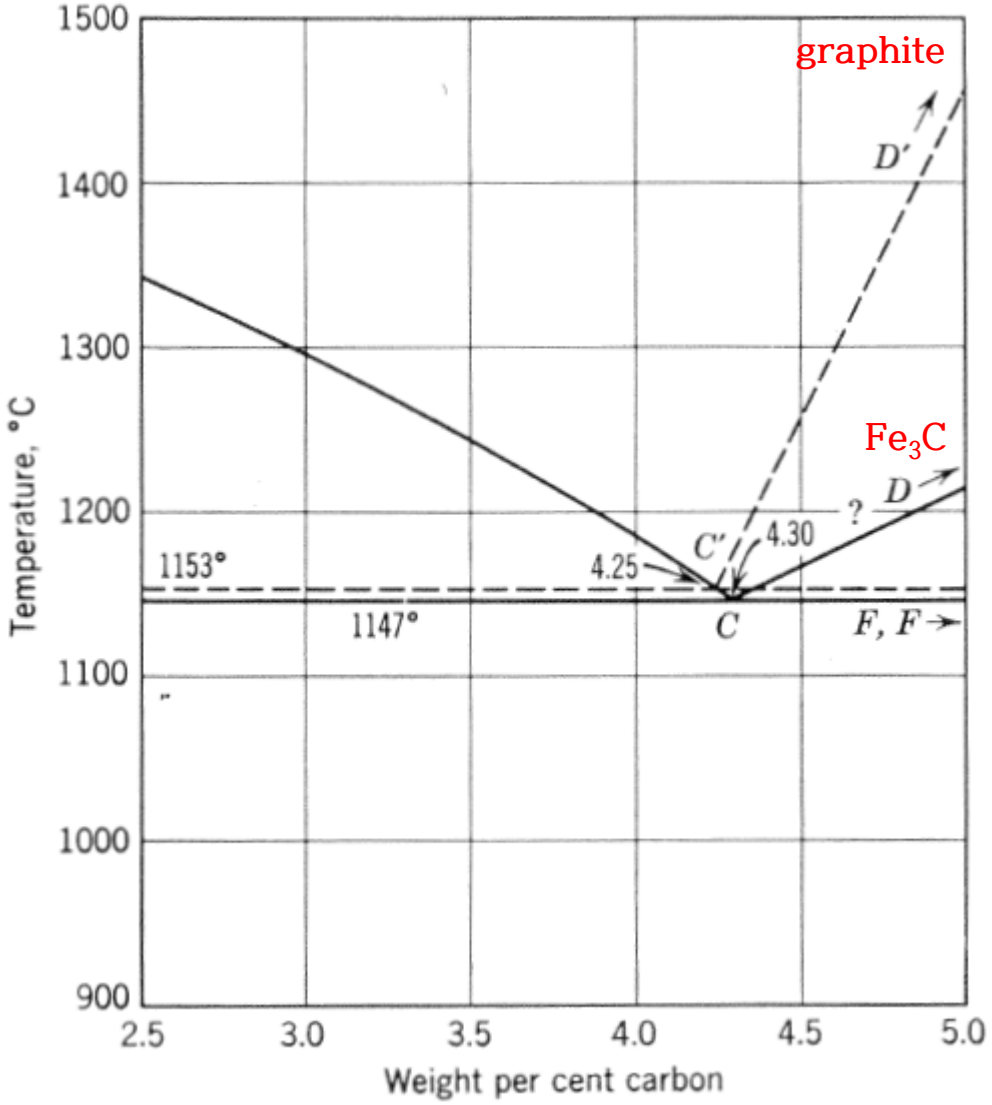

Fig. 6.35. Eutectic region of the iron carbon system.

* Addition effects of other elements

① Si → $T_E^{graphite}$ ↑ / $T_E^{Cementite}$ ↓

② Cr: decreasing the temperature rage where graphite is formed

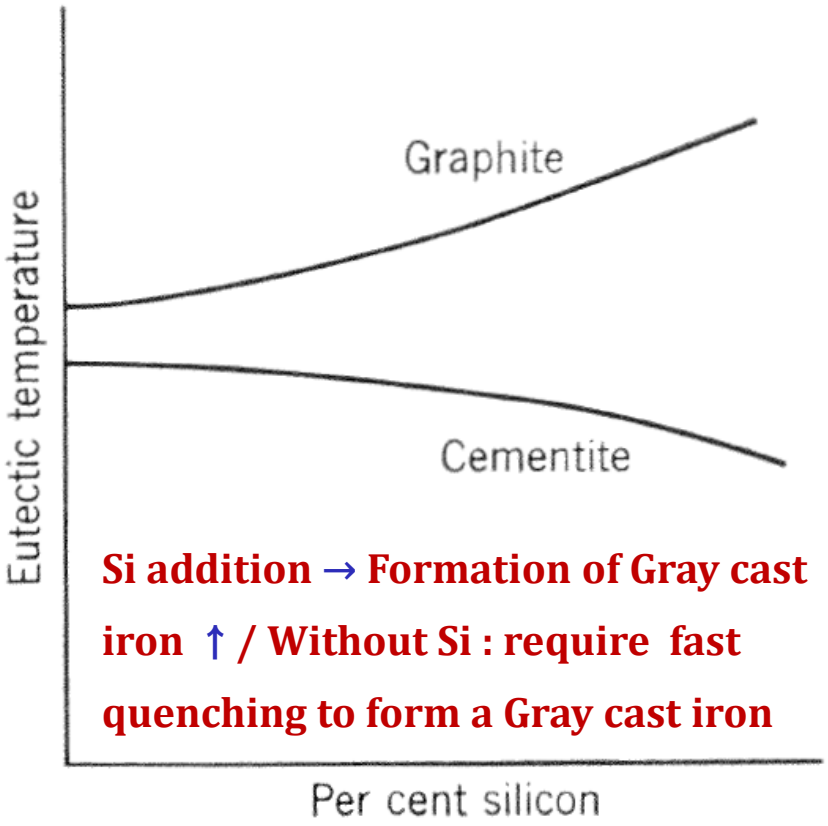

Si addition → Formation of Gray cast iron ↑ / Without Si : require fast quenching to form a Gray cast iron

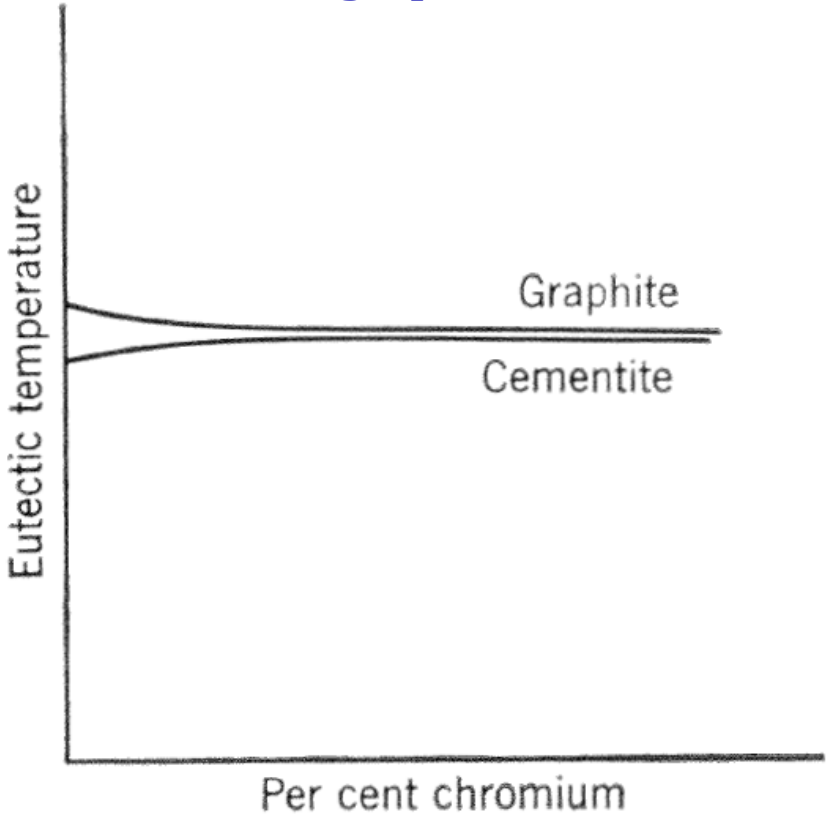

Fig. 6.36. Effect of third component on the eutectic temperatures (schematic). (a) Silicon type, (b) chromium type.

* Graphite morphology

2D: separated flake shape

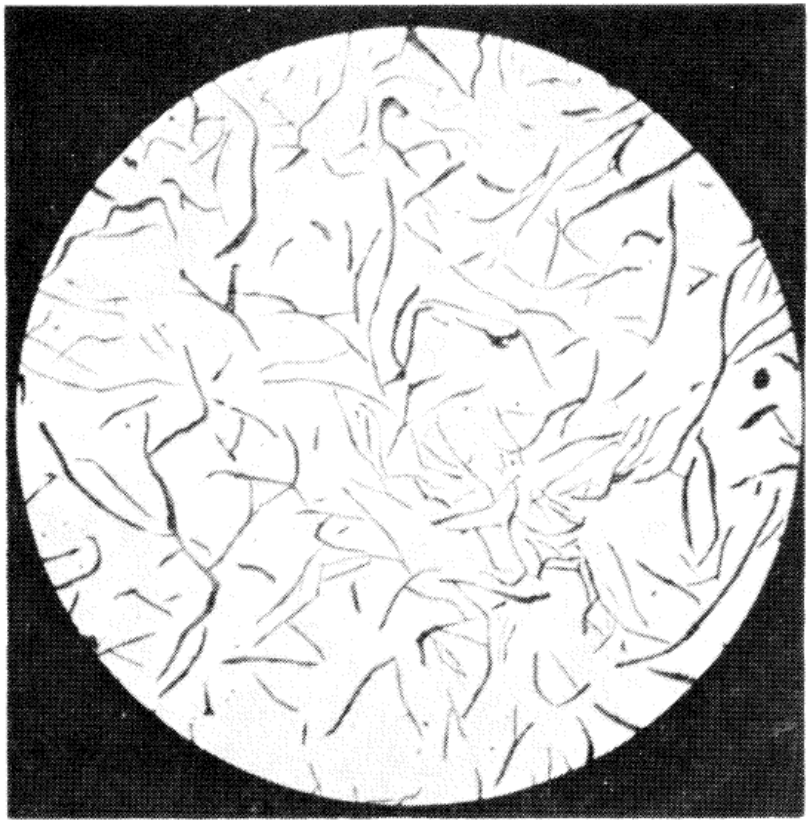

(a)

Fig. 6.37. Graphite in cast iron. (a) Nodular,

3D: Continuous flake shape after dissolving out the iron

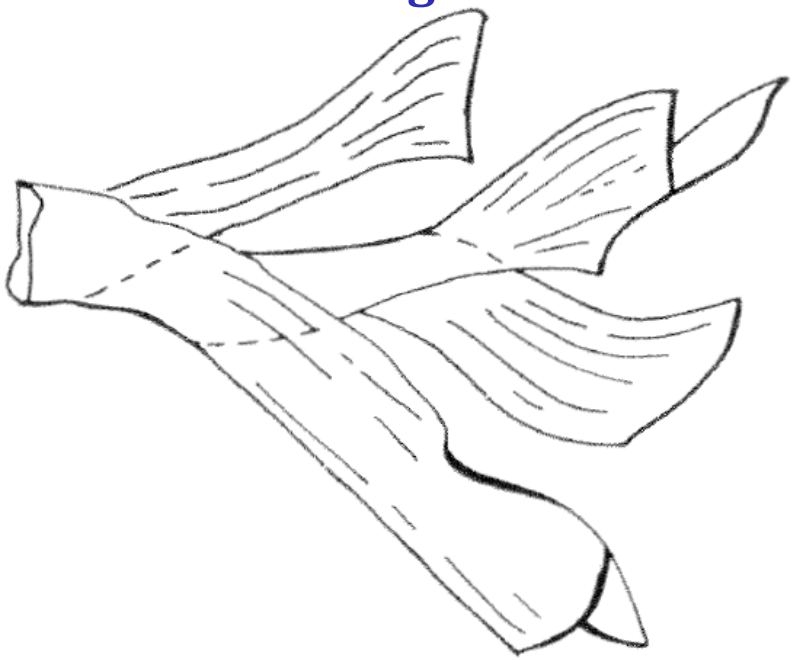

Fig. 6.38. Continuous graphite flake (schematic).

- **Spheroidal graphite:** Similar to the Si shape control method used for Al-Si for improving mechanical properties, a small amount of Cerium was added to gray cast iron

Continuous flake → formation of discrete spherulet

* Spherulitic graphite morphology

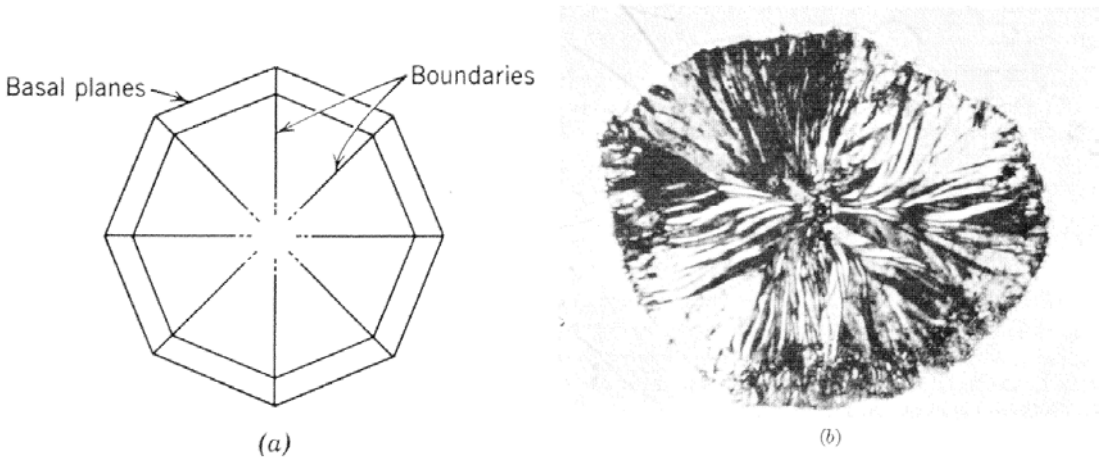

Fig. 6.39. Spherulet of graphite. (a) Schematic, (b) photomicrograph.

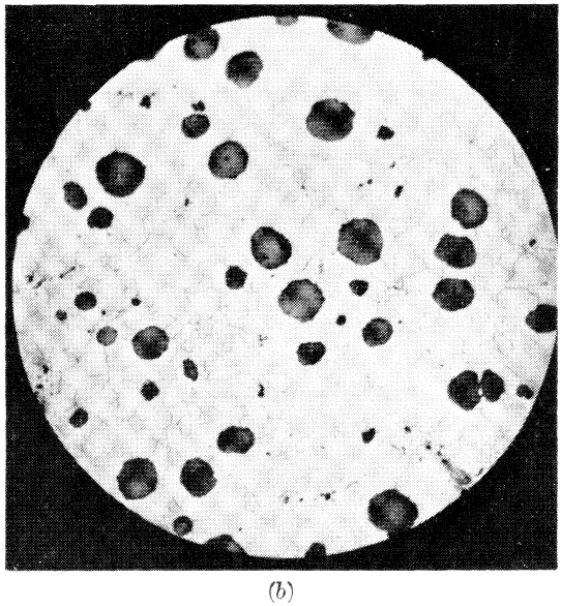

Fig. 6.37. Graphite in cast iron. (b) spherioidal.

- Orientation: everywhere such that the basal plane of the structure (which is the low E surface) faces the melt.→ highly polyhedral structure
- Probably most stable form, energetically (combine a low surface area → spherical shape)
- appears during long-term heat treatment of cast iron (malleableizing) : most stable configuration will be approached.
- Development of Spherulitic form = very low contents of sulfur in Iron melt/ Addition of spherodizing agent (Ce or Mg) → combining with sulfur / Addition of inoculant (Si) → produce graphite rather than cementite

Production of Cast Irons

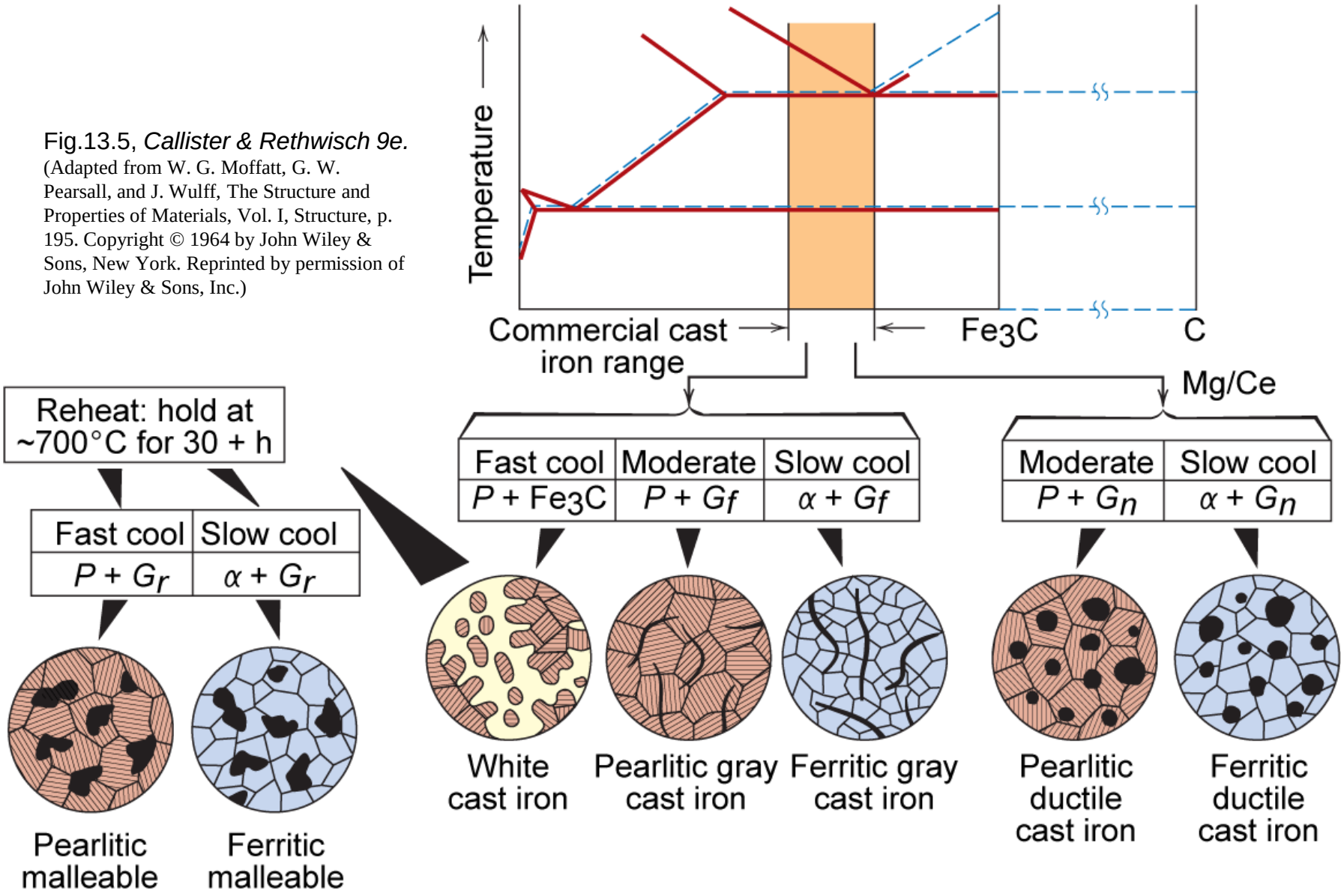

Fig.13.5, *Callister & Rethwisch 9e.*
(Adapted from W. G. Moffatt, G. W. Pearsall, and J. Wulff, The Structure and Properties of Materials, Vol. I, Structure, p. 195. Copyright © 1964 by John Wiley & Sons, New York. Reprinted by permission of John Wiley & Sons, Inc.)

Types of Cast Iron

Gray iron

- graphite flakes
- weak & brittle in tension
- stronger in compression
- excellent vibrational dampening
- wear resistant

Ductile iron

- add Mg and/or Ce
- graphite as nodules not flakes
- matrix often pearlite – stronger but less ductile

Figs. 13.3(a) & (b), *Callister & Rethwisch 9e.* [Courtesy of C. H. Brady and L. C. Smith, National Bureau of Standards, Washington, DC (now the National Institute of Standards and Technology, Gaithersburg, MD]

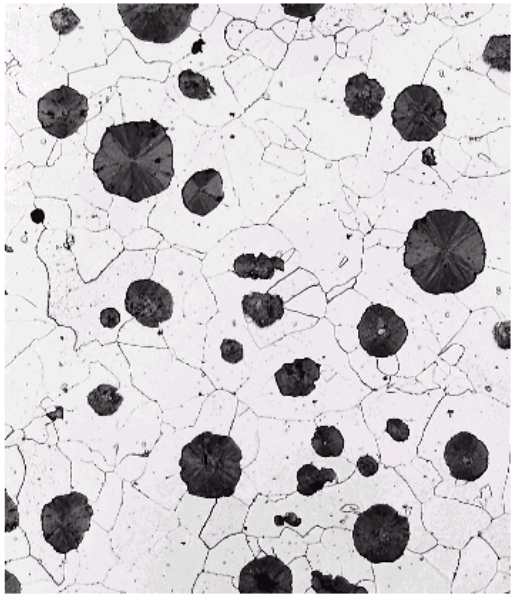

Types of Cast Iron (cont.)

White iron

- < 1 wt% Si
- pearlite + cementite
- very hard and brittle

조밀흑연주철

Figs. 13.3(c) & (d), *Callister & Rethwisch 9e.*

Courtesy of Amcast Industrial Corporation

Malleable iron

- heat treat white iron at 800-900°C
- graphite in rosettes (장미상 조직)
- reasonably strong and ductile

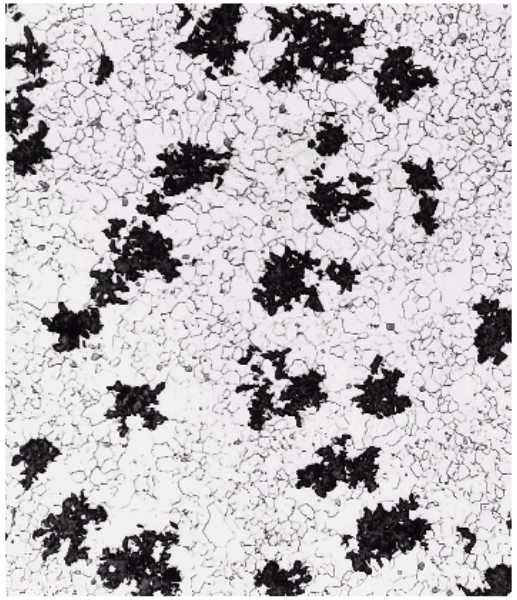

Reprinted with permission of the Iron Castings Society, Des Plaines, IL

Types of Cast Iron (cont.)

Compacted graphite iron

- relatively high thermal conductivity
- good resistance to thermal shock
- lower oxidation at elevated temperatures

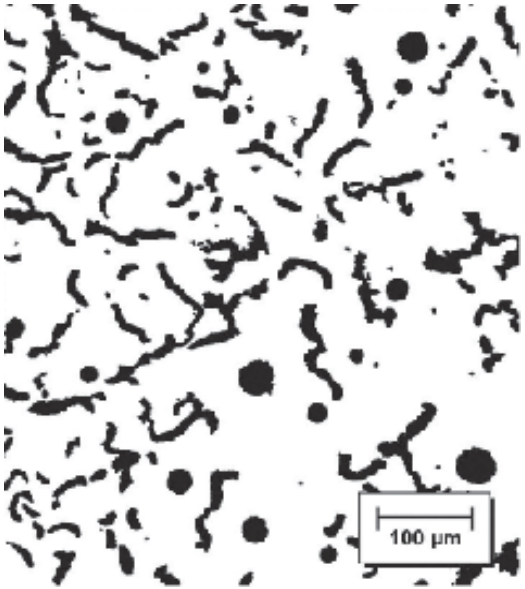

Courtesy of Sinter-Cast, Ltd.

Fig. 13.3(e), *Callister & Rethwisch 9e.*

13) Peritectic Solidification

: Occurs when two liquidus lines intersect with a slope of the same direction

*** Eutectic reaction: One liquid is balanced with two solid phases at a fixed composition and temperature**

*** Peritectic reaction l+α→β**

→ complete equilibrium
: Only possible under equilibrium solidification conditions.

→ at peritectic temperature
during cooling, Liquid composition P / α composition S

① C_0 → l+α→β

② C_1 or C_2 → Primary α or liquid + β

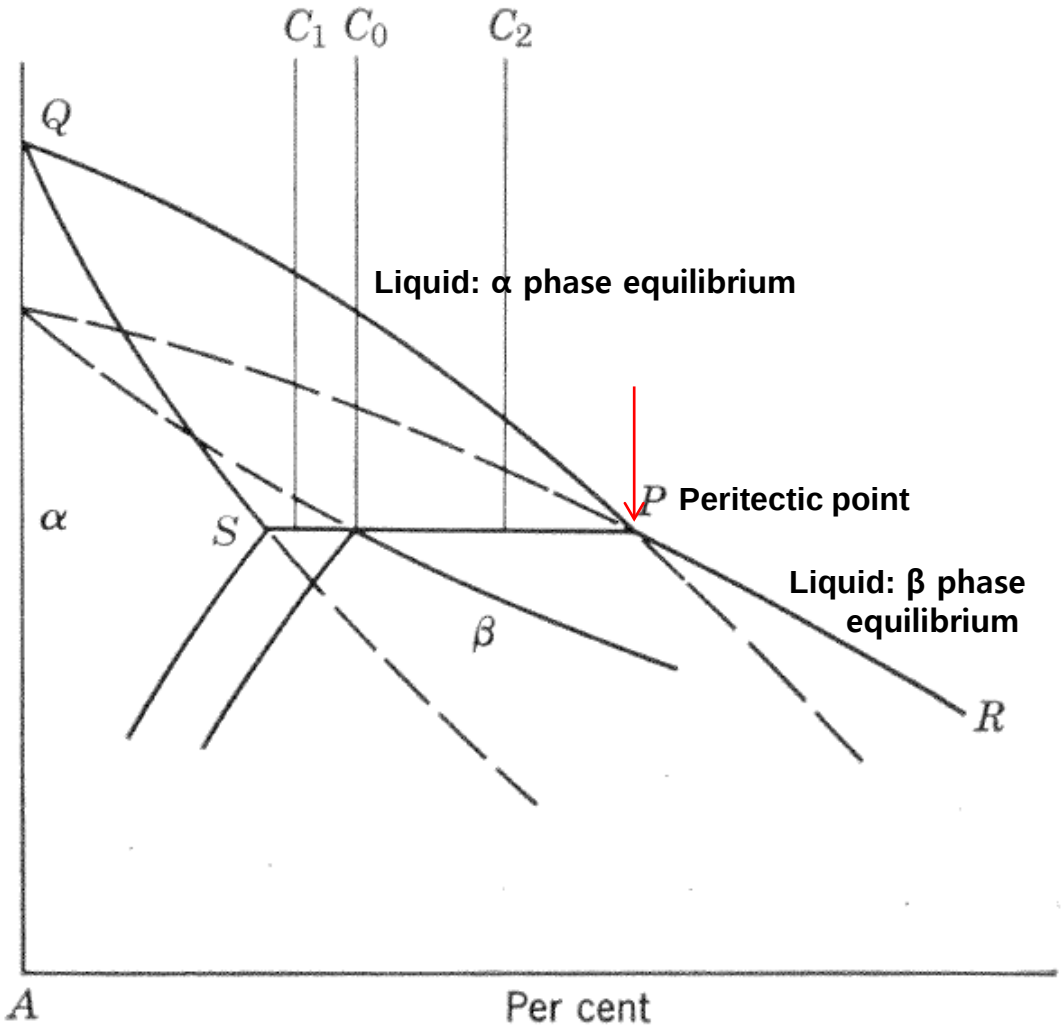

Fig. 6.40. Peritectic system, showing equilibrium phase boundaries ——— and nonequilibrium phase boundaries – – –.

* L + α → β is a very slow reaction except for the initial state, because liquid and α are separated by β

→ Diffusion must always occur for reaction to continue

→ When β is thickened (diffusion distance increases), the reaction slows down.

* Solidification and microstructure that develop as a result of the peritectic reaction

→ Unlike eutectic, peritectic does not grow into lamellar structure.

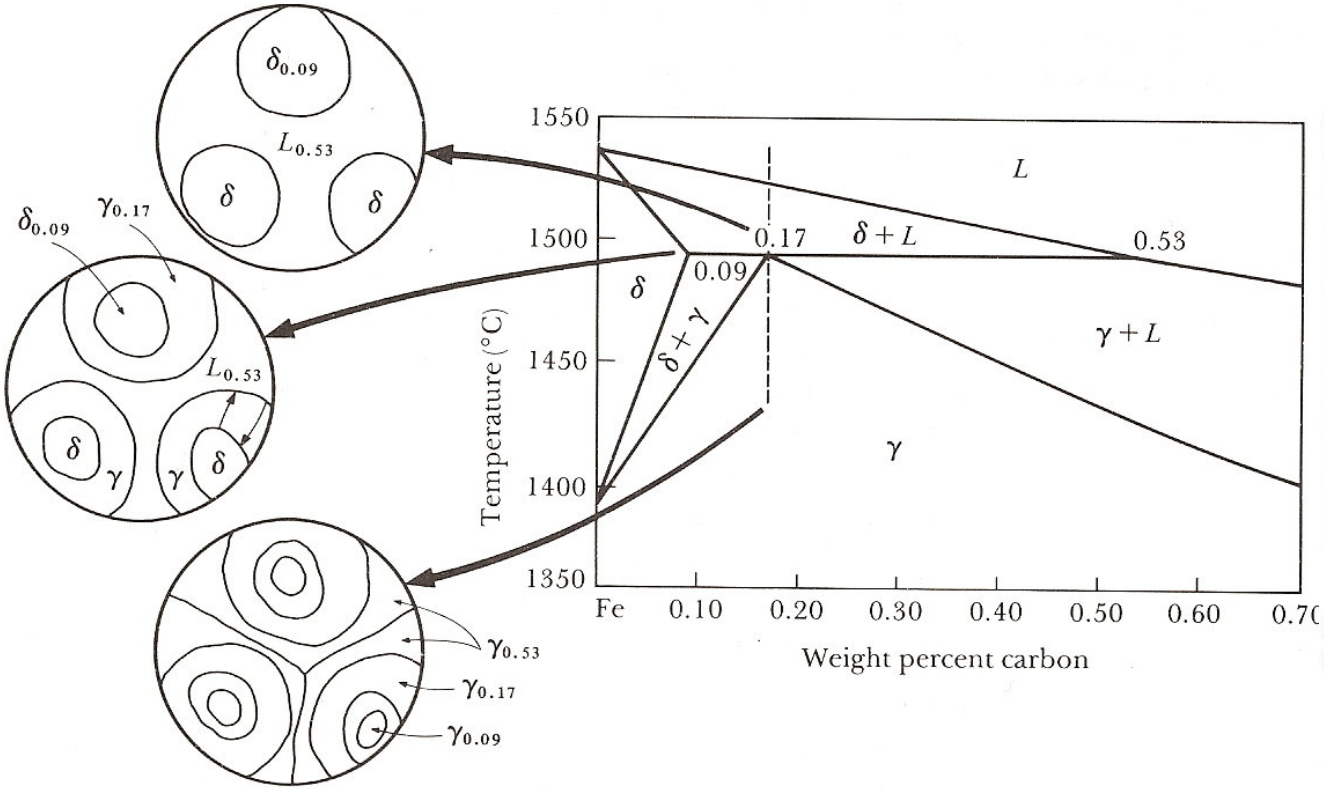

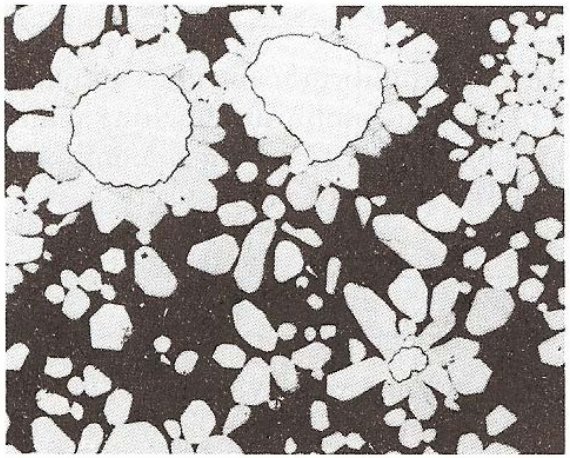

FIGURE 10-24 The peritectic reaction in a Cd-10% Cu alloy begins when rounded

* L + α → β is a very slow reaction except for the initial state, because liquid and α are separated by β

* Uhlmann and Chadwick: Ag-Zn peritectic experiment

→ Peritectic melt of composition M_1 :

→ below T_3, β matrix + massive α dendrites

→ Dendrite α phase remaining at wide composition range and growth speed

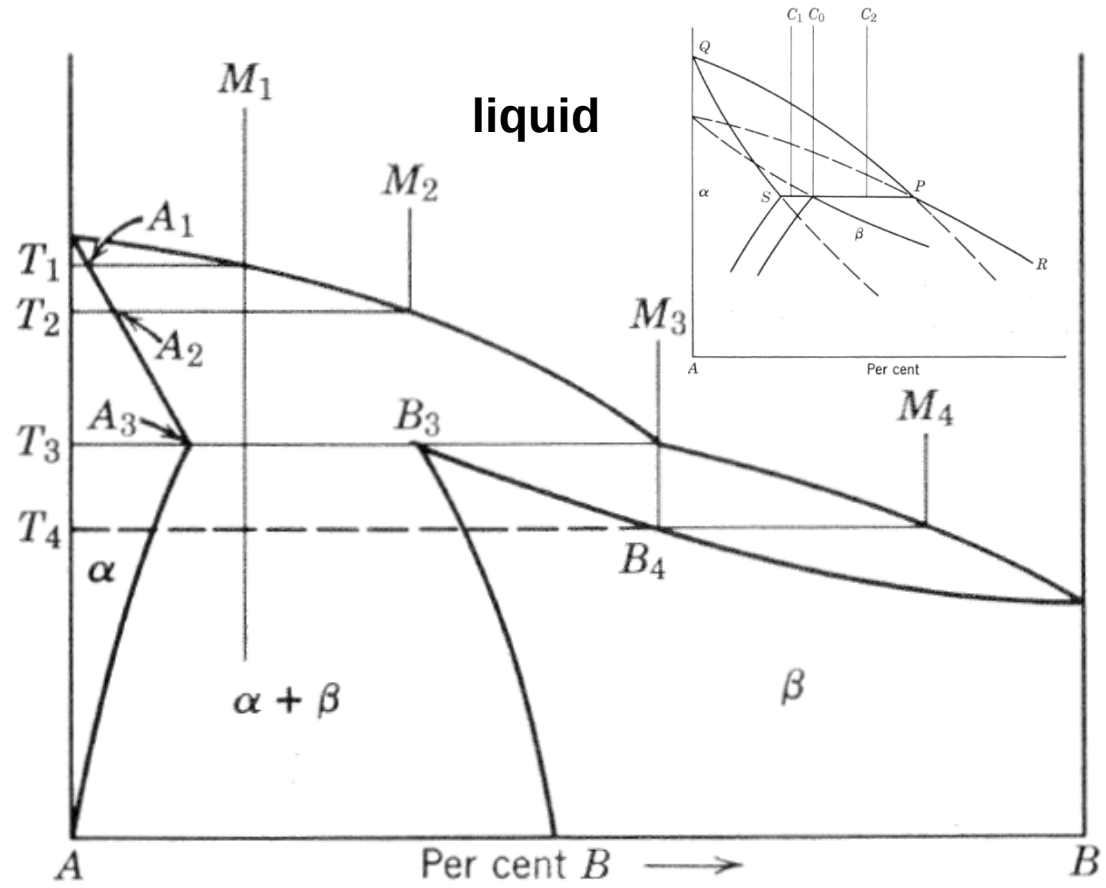

Fig. 6.41. Peritectic system.

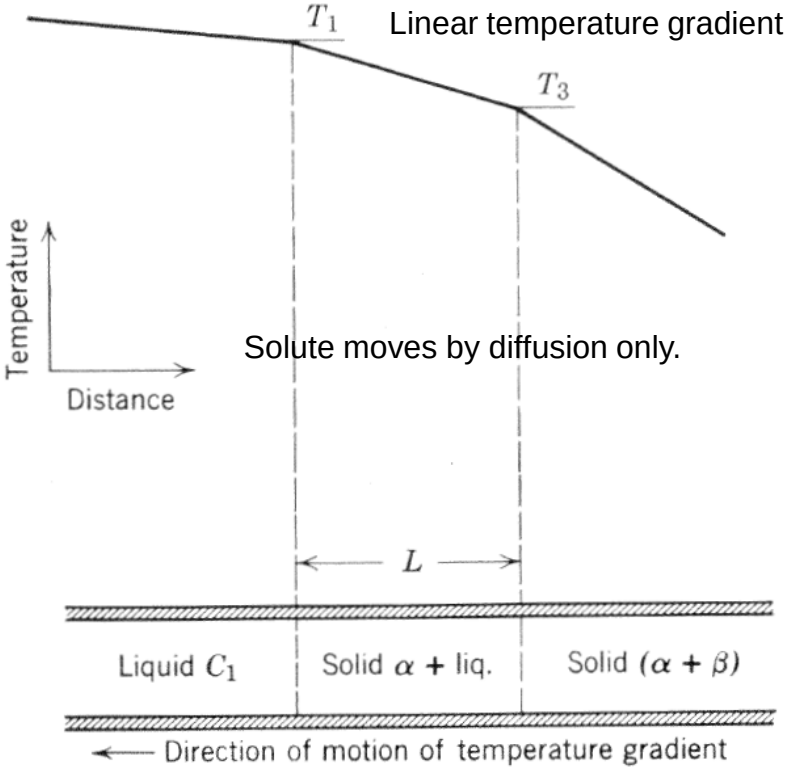

Fig. 6.42. Solidification of a peritectic in a temperature gradient.

*** L + α → β is a very slow reaction except for the initial state, because liquid and α are separated by β**

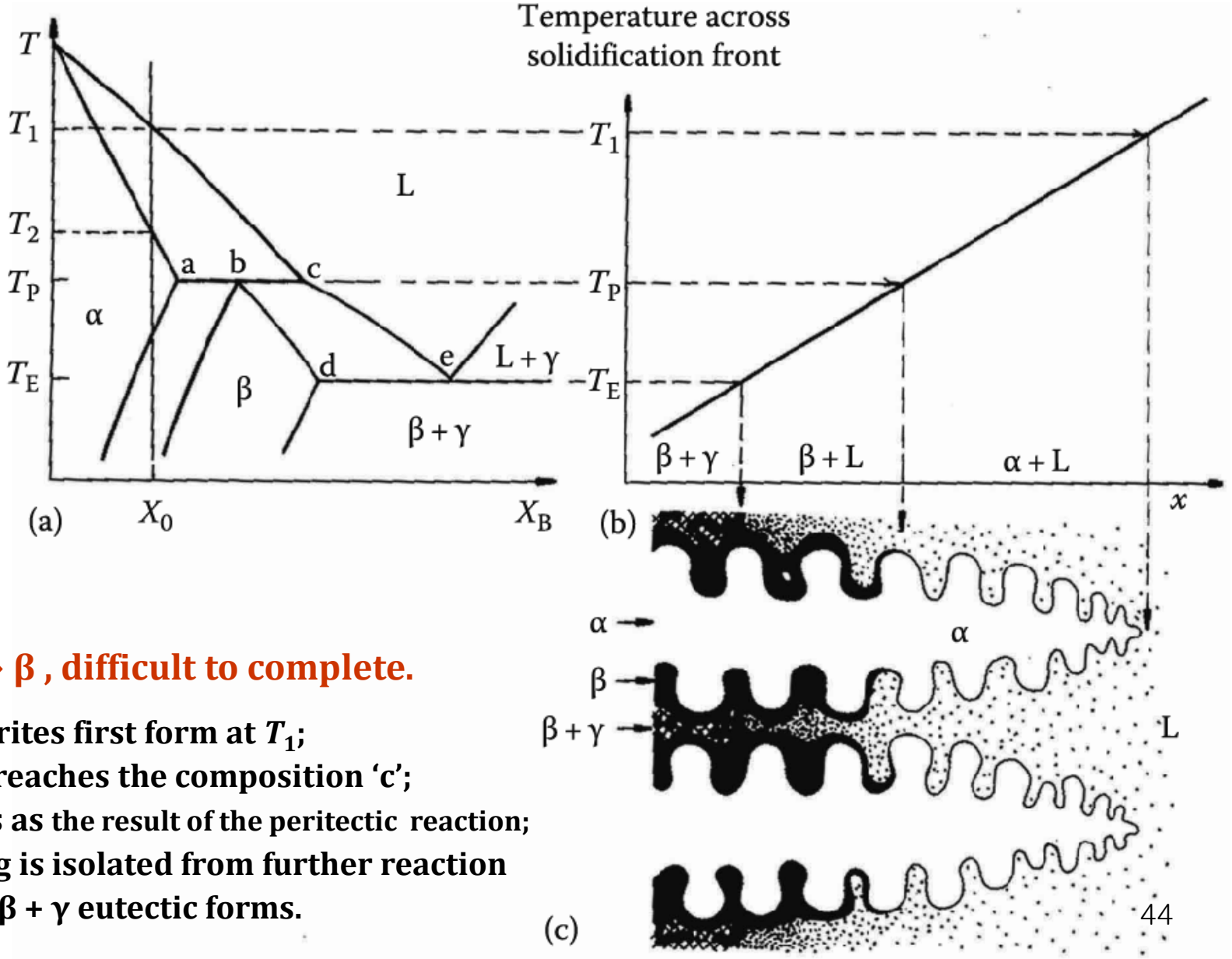

- **L + α → β , difficult to complete.**

- **α dendrites first form at T_1;**
  Liquid reaches the composition 'c';
  β forms as the result of the peritectic reaction;
  α coring is isolated from further reaction
  finally β + γ eutectic forms.

6.4. Solidification in the presence of a solid phase

- If liquid metals contain particles of solid in suspension; their distribution in the resulting solid influence dislocation content (page 58) or directly the mechanical properties. → relevant to consider the interaction btw an advancing S-L interface and solid particles in the liquid.

- **Three factors that may influence the final location of a particle**

(1) If "density" of particle is different from that of liquid: particle ~ float or sink

- Particle behavior dominated by its buoyancy (positive or negative)

: depends on density difference and the size and shape of the particle

Ex) A particle (sufficiently small) will remain in suspension indefinately as a result of its Brownian motion even if its density is substantially different from that of the liquid. The actual size for effective Brownian motion depends on the density difference, but in general is of the order of 0.1 μm.

*** Rate (B) of ascent or descent for large particle: by Stokes formula**

① **Sphere,**

$$B = \frac{2}{9}\frac{gr^2(D_1 - D_2)}{\eta}$$

r = 1 μm particle/ Density difference, Δd=2 gm/cm^3

→ B = order of 10^{-4} cm/sec

② **For non-spherical shapes, the value of B is smaller because a particle always tends to orient itself so that it offers the max. resistance to its own motion through the liquid.**

(2) Second factor = "Fluid motion"_ generated as the liquid enters the mold

large enough to maintain in suspension particles that would sink or float in a stationary liquid

: persist for a considerable time before it gives way to convection caused by thermal and composition gradient.

(3) Third factor = "Interface speed" : Although there may be some vertical separation due to flotation or sedimentation, and some radial separation resulting from centrifugal forces, the smaller particles may remain suspended with a nearly random distribution.

→ ∴ The final distribution in the solid depends on whether a particle is "trapped" in situ by the advancing S-L interface or whether it is pushed ahead as the interface moves forward.

→ Experiments (Uhlmann & Chalmers) : some nonmetallic system

1) Fast rate of advancing interface (>critical velocity, CV) : particles are "trapped".

(ex) MgO particle in Orthoterphenyl: critical velocity_about 0.5 um/sec

2) Although the CV varies from 0 to 2.5 μm/sec depending on the type of matrix and particle, no definitive composition and crystallographic effects have been identified.

3) (surprising feature) Critical velocity is independent of particle size change.

→ This CV (up to 2.5 μm / sec or 1 cm / hr) is very slow compared to most practical solidification or crystal growing processes and it is very unlikely that dispersed particles can change the solidification process if they have a similar CV in metal and semiconductor.

* Solidification of a liquid in a porous solid

: Little attention has been paid to the solidification of a liquid metal that is contained in interconnected channels in a porous solid that is chemically inert to the solidifying liquid.

(ex) Nonmetallic system: Freezing of water in Soil → Induce "frost heaving load"

- These forces arise not because water expands on freezing, but because a water layer persists between ice and solid particles. As ice is formed, more water is drawn into the region of contact to replace what has frozen. This water in turn stars to freeze, causing more water to be "sucked" in, and forcing the existing ice away from the soil particle.

→ Preference, energetically, for the existence of a liquid layer btw the two solids

→ *A liquid metal contained in a porous matrix may have a similar surface E relationship*, in which case very large forces could be exerted, tending to disrupt the matrix.